AD-A090 172   BLOCK ENGINEERING INC CAMBRIDGE MA   F/G 20/14
SUBMILLIMETER WAVE HIGH RESOLUTION ATMOSPHERIC TRANSMISSION MEA--ETC(U)
DEC 78 N J JOHNSON, T G QUINN, J KAUFFMAN   DAAB07-78-C-2438
UNCLASSIFIED BEI-78-772   NL

1 OF 1
AD
A090 172

END
DATE
FILMED
11-80
DTIC

LEVEL II

AD A090172

BLOCK
ENGINEERING, INC

Cambridge, Mass. 02139

80 9

14 BEI-78-772

1 SUBMILLIMETER WAVE HIGH RESOLUTION
ATMOSPHERIC TRANSMISSION
MEASUREMENTS STUDY.

9 FINAL TECHNICAL REP[redacted]T.
20 Apr[redacted]78-[redacted] 20 Jan[redacted]79

Contract No. 15 DAAB07-78-C-2438

12 66

Submitted to:

U.S. Army Electronics Command
Fort Monmouth, N.J.

11 Dec 79

Prepared by:

10 N.J.E. Johnson, T.G. Quinn III
J. Kauffman

BLOCK ENGINEERING, INC.
19 Blackstone Street
Cambridge, Massachusetts

059070

Block Engineering, Inc.

TR ECOM-
DECEMBER 1978

Reports Control
Symbol OSD-1366

BEI-78-772

SUBMILLIMETER WAVE HIGH RESOLUTION ATMOSPHERIC TRANSMISSION MEASUREMENTS STUDY

FINAL TECHNICAL REPORT
20 April 1978 to 20 January 1979

CONTRACT NO. DAAB07-78-C-2438

Prepared by

N.J.E. Johnson, T.G. Quinn III,
J. Kauffman

BLOCK ENGINEERING, INC.
19 Blackstone Street
Cambridge, Massachusetts

For

U.S. ARMY ELECTRONICS COMMAND, FORT MONMOUTH, N.J.

centimeters to -1, 3000

ABSTRACT

The measurement of atmospheric transmission under various weather conditions at submillimeter wavelengths was carried out using an interferometer modulator transmitter and cooled composite bolometer receiver over transmission paths to 100 meters. Measurements were made in the laboratory and outside, with relative humidity to 97%. Spectral resolution was better than 0.1 cm^{-1}, and spectral range extended from 100 microns to just beyond 1.0 millimeter. Although some channeling was observed in earlier spectra, this effect was removed in later measurements, and data quality is generally excellent.

0.1 1/cm

TABLE OF CONTENTS

Section		Page
1.	INTRODUCTION	1
2.	INSTRUMENTATION	2
2.1	Interferometer/Transmitter	2
2.2	Radiometer/Receiver	3
2.3	Electronics	11
2.4	Data System	11
3.	MEASUREMENTS	12
3.1	Preliminary Measurements	12
3.2	Interior Measurements	12
3.3	Exterior Measurements	12
3.4	Data Reduction	13
4.	DATA	15
4.1	Spectra	21
4.2	Discussion	52
5.	CONCLUSIONS	55
5.1	Further Measurements	55
5.2	Instrument Modifications	55
5.3	Measurement Scheduling	57
	BIBLIOGRAPHY	58

LIST OF FIGURES

Figure		Page
2.1-1	Eight inch receiver and twelve inch mirror.	4
2.1-2	Looking into transmitter from 12 inch folding mirror.	5
2.2-1	0.8 mm Crystalline Quartz with Garnet Powder at 4°K.	7
2.2-2	0.8 mm Crystalline Quartz, 300°K w/a-r coating.	8
2.2-3	(5-10μ) Diamond Powder on Polyethylene Film 330°K.	9
2.2-4	1.5 mm TPX, 300°K, #600 Finish, Wedged.	10
4.0-1	Zero Path Setup, Transmitter and Receiver Head-on.	20
4.1-1	Arc Lamp Spectrum with 25 Micron Beamsplitter.	22
4.1-2	Arc Lamp Spectrum with 50 Micron Beamsplitter.	23
4.1-3	Arc Lamp Spectrum with 125 Micron Beamsplitter.	24
4.1-4	Background Spectrum with 125 Micron Beamsplitter.	25
4.1-5	Arc Lamp Spectrum with Background Spectrum Subtracted.	26
4.1-6	Arc Lamp Interferogram.	27
4.1-7	Non-Normalized Spectrum.	28
4.1-8	Fudged Reference Spectrum.	29
4.1-9	Zero Path (Head-on) Spectrum, 97% R.H., 15°C.	31

LIST OF FIGURES (Continued)

Figure		Page
4.1-10	Background (with mirror) Spectrum, 97% R.H., 15°C.	32
4.1-11	Zero Path (Folded) Spectrum, 90% R.H., 16°C.	33
4.1-12	12.5 Meter Spectrum, 97% R.H., 16°C.	34
4.1-13	25 Meter Spectrum, 97% R.H., 16°C.	35
4.1-14	50 Meter Spectrum, 97% R.H., 16°C.	36
4.1-15	100 Meter Spectrum, 90% R.H., 16°C.	37
4.1-16	Zero Path (Folded) Spectrum, 50% R.H., 2°C.	38
4.1-17	12.5 Meter Spectrum, 46% R.H., 3°C.	39
4.1-18	25 Meter Spectrum, 46% R.H., 3°C.	40
4.1-19	50 Meter Spectrum, 39% R.H., 4°C.	41
4.1-20	100 Meter Spectrum, 39% R.H., 4°C.	42
4.1-21	Zero Path (Folded) Spectrum, 50% R.H., 4°C.	43
4.1-22	12.5 Meter Spectrum, 50% R.H., 3°C.	44
4.1-23	25 Meter Spectrum, 46% R.H., 3°C.	45
4.1-24	50 Meter Spectrum, 39% R.H., 4°C.	46
4.1-25	100 Meter Spectrum, 39% R.H., 4°C.	47
4.1-26	12.5 Meter Ratio, 46% R.H., 3°C.	48
4.1-27	25 Meter Ratio, 46% R.H., 3°C.	49
4.1-28	50 Meter Ratio, 39% R.H., 4°C.	50
4.1-29	100 Meter Ratio, 37% R.H., 4°C.	51

1. INTRODUCTION

This final technical report is submitted in partial fulfillment of the requirements of Contract No. DAAB07-78-C-2438 (CLIN 0002, CDRL H001) with the U.S. Army Electronics R&D Command at Fort Monmouth, New Jersey. This work was performed for Dr. Rudolph Buser and Dr. Robert Rohde of that organization, and involved the preparation of instrumentation and the measurement of transmission through the atmosphere at submillimeter wavelengths under varying atmospheric conditions.

Instrumentation was prepared and measurements were made with spectroradiometric sensitivity extending from 100 microns to above 1 millimeter wavelengths. Data were obtained both in the laboratory and outside, for transmission paths up to 100 meters long and in conditions of up to 97% relative humidity. Spectra were prepared for all measurements and calibrations, and ratio spectra were obtained indicative of atmospheric transmission.

The results were very encouraging. Peak signal-to-r.m.s. noise of 50:1 was obtained over 100 meter paths for 512 scan integrations at 0.12 cm^{-1} spectral resolution (apodized). It is possible that anomalous features were observed in the region at 10 cm^{-1} or beyond, as noted by Moffat et al (1977), Gebbie et al (1968), and others, but additional measurements and analysis are required.

Further measurements with wire grid beamsplitters, larger telescope mirrors, and a larger detector are needed to reduce interference and diffraction losses at the longer wavelengths. These losses prevent the clear definition of the possible anomalous absorptions, especially below 10cm^{-1}. It is also desirable that measurements be made at a location where complete meteorological data,* including aerosol scattering measurements, can be obtained to support the spectrometric data.

NOTE: Mixed English and metric units are used in this report, reflecting present U.S. commercial practice in specifying optics and also in all cases as original data measurements were recorded.

2. INSTRUMENTATION

The basic instrumentation used in these measurements was provided by Block Engineering, modified as necessary for the program. This instrumentation included a mercury arc lamp source, interferometer modulator, transmitter telescope, receiver telescope, detector, electronics, and data processing system.

2.1 INTERFEROMETER/TRANSMITTER

The high frequency modulation of radiation transmitted over the measurement path is the only effective way to eliminate background radiation phenomena in the submillimeter wave region. Interferometric modulation of source radiation was obtained by mounting the source at the input of a Block Model 496 interferometer. The output of the interferometer is modulated so that radiation frequencies are produced according to the relation

$$f = \dot{B}/\lambda \quad \text{Hz}$$

where $\dot{B}$ is the interferometer retardation rate (10.12 cm/sec) and λ is the wavelength of the radiation (cm). The spectral range of 100 microns to above 1 millimeter gave a frequency range of 100 to 1000 Hz in the transmitted beam, well above typical atmospheric fluctuation frequencies.

A blackbody radiation source was used in the preliminary measurements during system checkout, but a high pressure mercury arc lamp was installed for all later measurements, giving three times the radiance at 1 mm wavelength. The lamp used was a Phillips 125 watt mercury vapor lamp, operated at the focus of a fast off-axis collimating mirror designed to overfill the 2.25" × 1.88" limiting aperture in the interferometer.

The interferometer provided 8.3 cm of retardation, offset to give an 8.0 cm one-sided interferogram. This provides better than 0.1 cm^{-1} spectral resolution in conjunction with the apodization function used in processing the data. The helium-neon laser in the interferometer provided the sampling reference for the digitization and storage of received signal interferograms, accurate to a fraction of the 0.6328 micron wavelength. A binary multiple of this wavelength was used to define the sampling interval, which was in this case 40.4992 microns (64X). Excellent spectral precision results from this technique, far better than the 0.1 cm^{-1} spectral resolution. Coaddition of scans to provide integration was possible, based on the white light reference built into the interferometer, giving identification of the reference retardation position to a fraction of the laser wavelength.

A mylar beamsplitter was used to produce interference, and various thicknesses were tested to determine the optimum for this experiment. The effect of a thin dielectric beamsplitter is to produce periodic dips in the spectral response, with the first null at zero frequency. Selection of a 50 micron beamsplitter thickness gave the second null at about 160 microns, and provided equivalent performance at 1.0 millimeter to a 125 micron beamsplitter which was examined. A 25 micron beamsplitter resulted in substantial loss in sensitivity at 1.0 millimeter wavelengths. In future measurements, the use of a free-standing wire grid beamsplitter would avoid the loss of data at 160 microns and improve efficiency beyond 1.0 millimeters. (Cost and delivery prevented use of this type of beamsplitter in the present work.)

The collimated output of the interferometer was focused by a plastic lens to provide an image plane prior to transmission through the telescope. This lens was made of a polyolefin based on poly 4 methyl pentene-1, known commercially under its trade name of TPX (Imperial Chemical Industries), and fabricated for this program by Infrared Laboratories, Inc. Since its refractive index is the same in the visible as in the submillimeter region, accurate optical alignment of the system was possible using the visible component of the arc lamp radiation.

The focused radiation was expanded to provide a collimated beam 12" in diameter using a cassegrain telescope with an f/2 primary and f/4 secondary mirrors. A field stop 0.95" in diameter was placed at the image plane, but the source image was smaller than this in one dimension, and the effective beam diameter is estimated at approximately 10 milliradians.

Gaseous nitrogen at low pressure was used to pressurize the air bearing in the interferometer. Cooling of the arc lamp housing was maintained by water pumped from a reservoir. In measurements outside, the transmitter and receiver were mounted side by side within a garage located at the company plant. A flat front surfaced mirror mounted on a tripod was used to reflect the beam back to the receiver. See Figure 2.1-1 and 2.1-2.

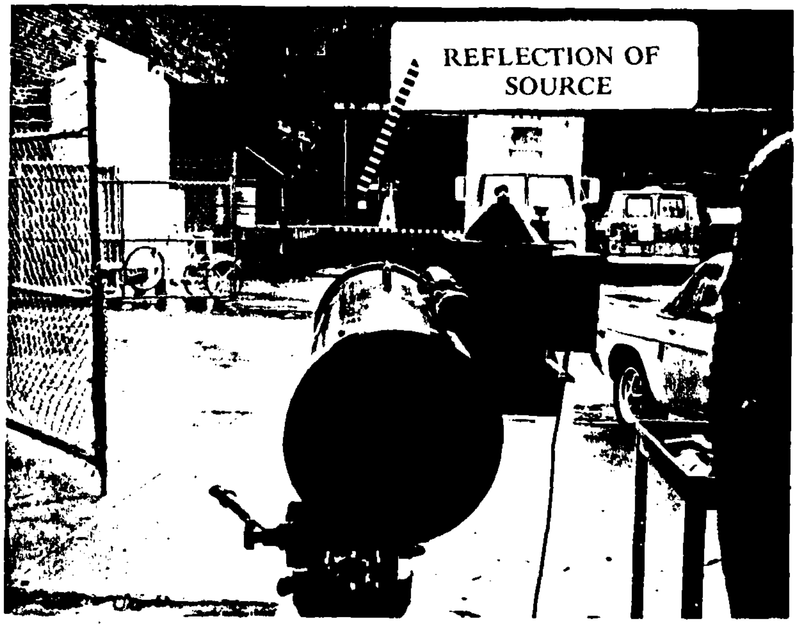

Figure 2.1-1. Eight inch receiver and twelve inch folding mirror.

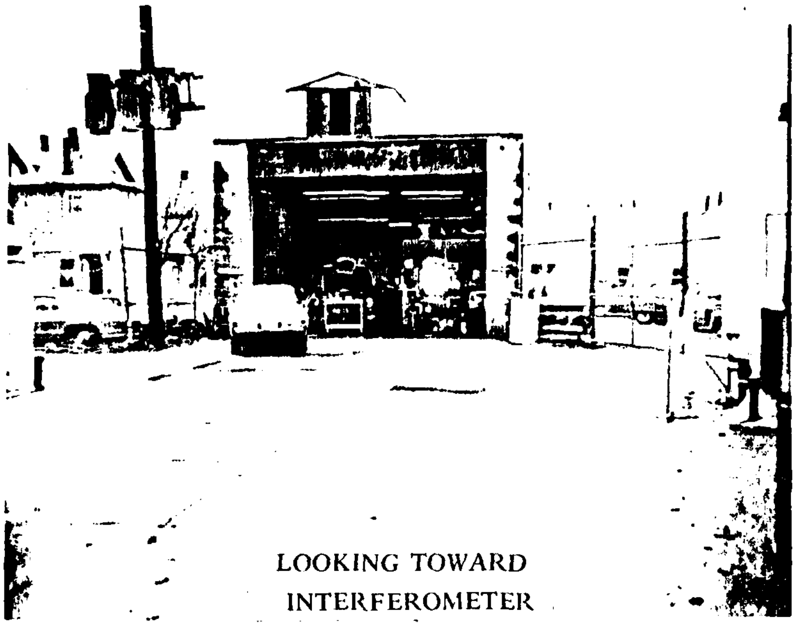

Figure 2.1-2. Looking into transmitter from 12 inch folding mirror.

2.2 RADIOMETER/RECEIVER

An in-house f/4 newtonian telescope with 8" diameter aperture was used to concentrate energy onto the detector through spectral filters and a field lens. The 3.0 mm square detector, made by Infrared Laboratories, Inc. for these measurements, was mounted with the field lens and filters in a liquid helium dewar, operating at 4.2°K. The receiver field of view was about 7 milliradians full angle as defined by the 6 mm aperture of the TPX field lens.

The detector used was a composite bolometer, in which a small gallium-doped germanium element is mounted on a thin sapphire plate coated with an absorbing metal film. This technique provides much lower heat mass for a given area compared with the gallium-doped germanium crystal alone, which provides the sensitivity to temperature necessary in detection. The noise-equivalent power of this detector was measured at Block to be 5.5×10^{-12} watts/Hz$^{1/2}$, but some atmospheric losses may have been present in this measurement despite careful purging of the apparatus, giving a poorer sensitivity than reported by Infrared Laboratories, Inc. The frequency response of the detector, extended to the 3db point, was 212 Hz, breaking at 6 db/octave beyond this frequency. Amplitude and phase distortion in the output signal resulting from the detector response are accurately and automatically compensated in the data processing through ratio elimination of the instrumental function. The corresponding decrease in signal-to-noise ratio at higher frequencies is more than compensated by the increase in source radiance at shorter wavelengths.

Two filters were used to eliminate all radiation short of 100 microns, and extensive baffling helped to minimize unnecessary radiation at the detector and thus improve its sensitivity. These filters used quartz as a substrate material and the 4.2°K filter was coated with garnet powder while the 300°K window filter was coated with diamond dust, sealed in plastic. The filters were originally plane-parallel elements, and consequently produced spectral channeling in the earlier spectra. This channeling resulted from multiple reflections within the elements, producing amplitude and phase variations with the angle between the transmitter and receiver optical axes and possibly with the transmission path length due to changes in effective throughput (area-solid angle product). Wedged filter elements were obtained and installed prior to the last measurement sequence, and channeling effects were not discernible in these data. The filter spectral responses are shown in Figures 2.2-1, 2.2-2, and 2.2-3, and the TPX lens transmittance is shown in Figure 2.2-4.

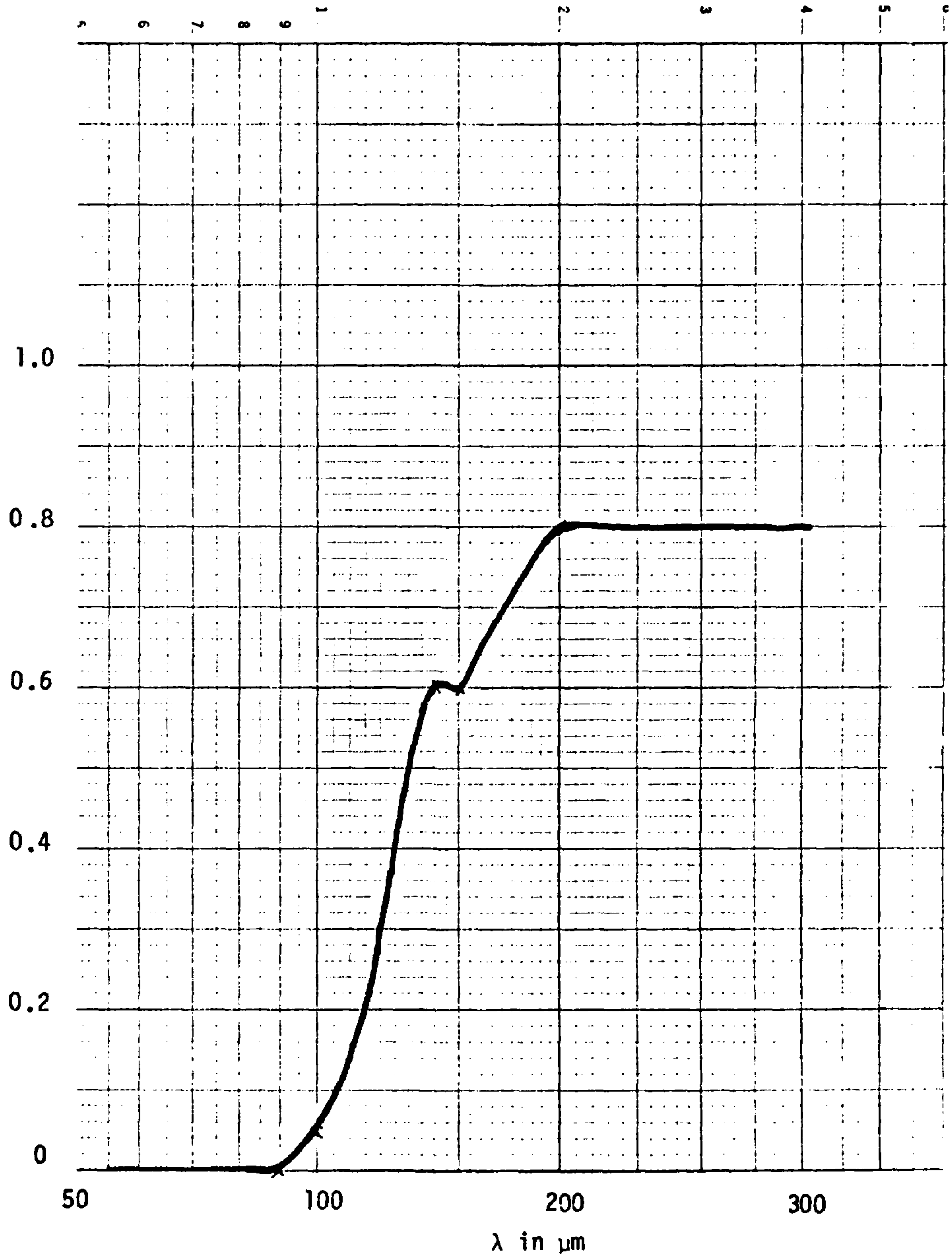

Figure 2.2-1. 0.8 mm Crystalline Quartz with Garnet Powder at 4°K.

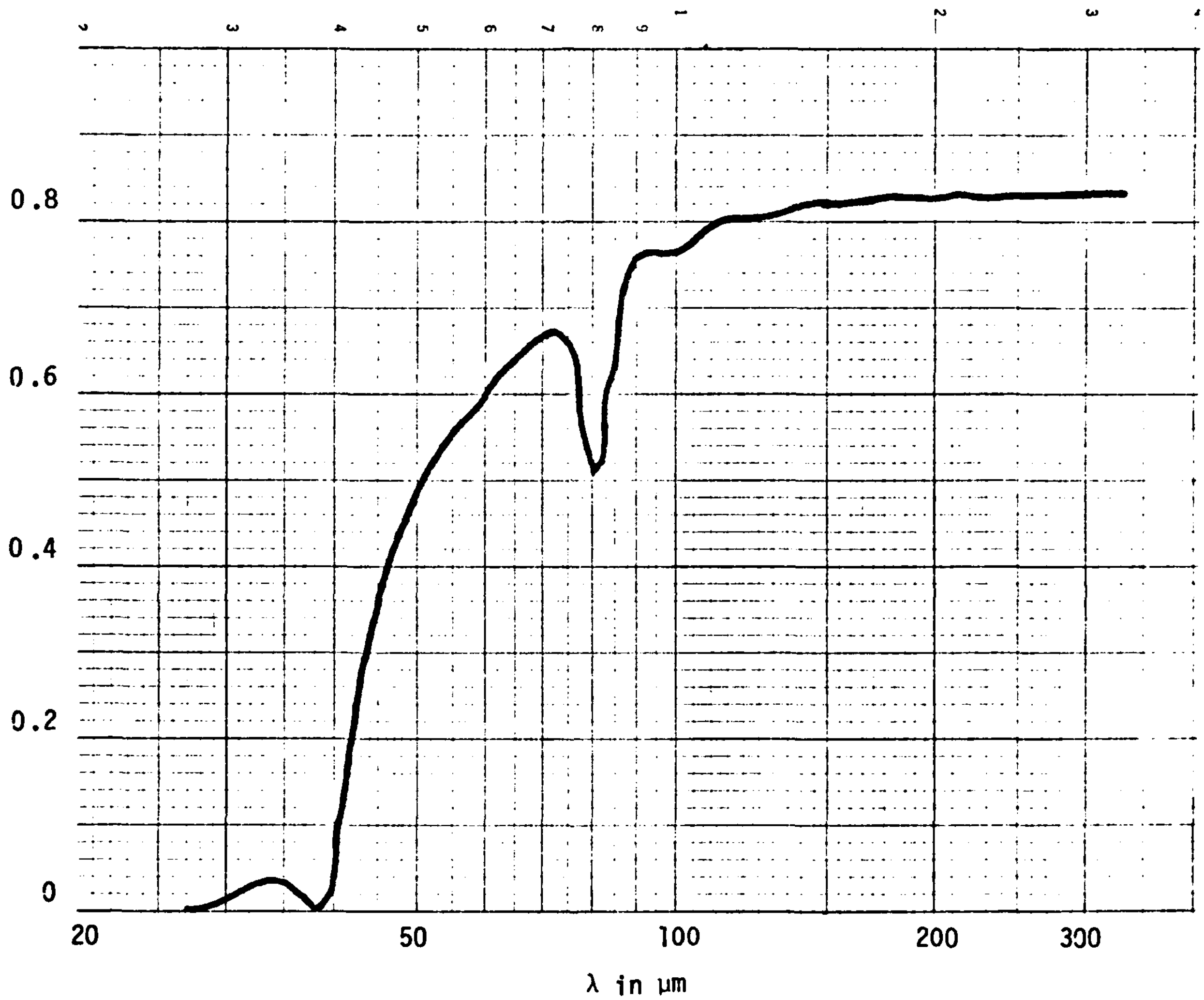

Figure 2.2-2. 0.8 mm Crystalline Quartz, 300°K w/A.R. coating.

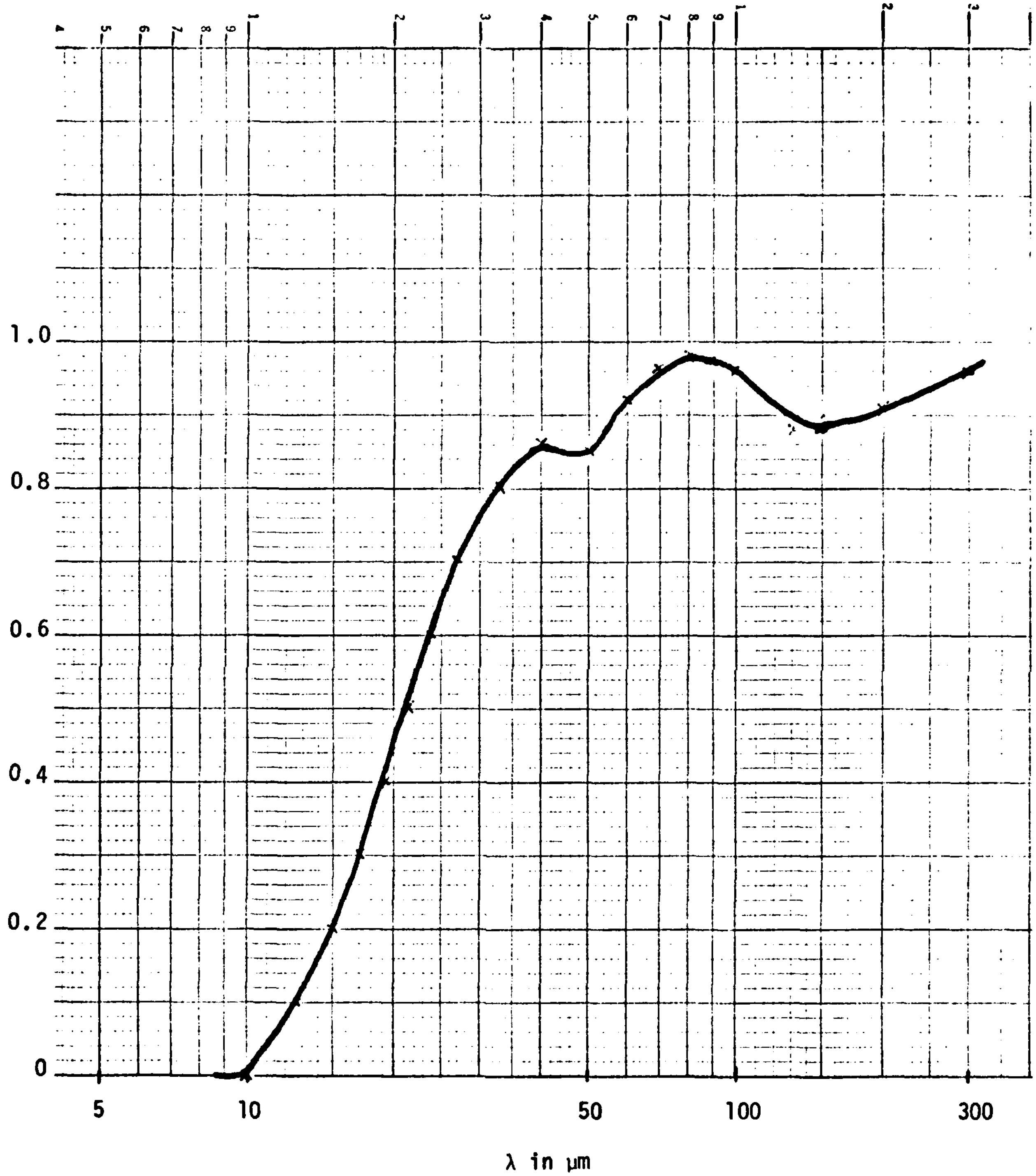

Figure 2.2-3. (5-10μ) Diamond Powder on Polyethylene Film 330°K.

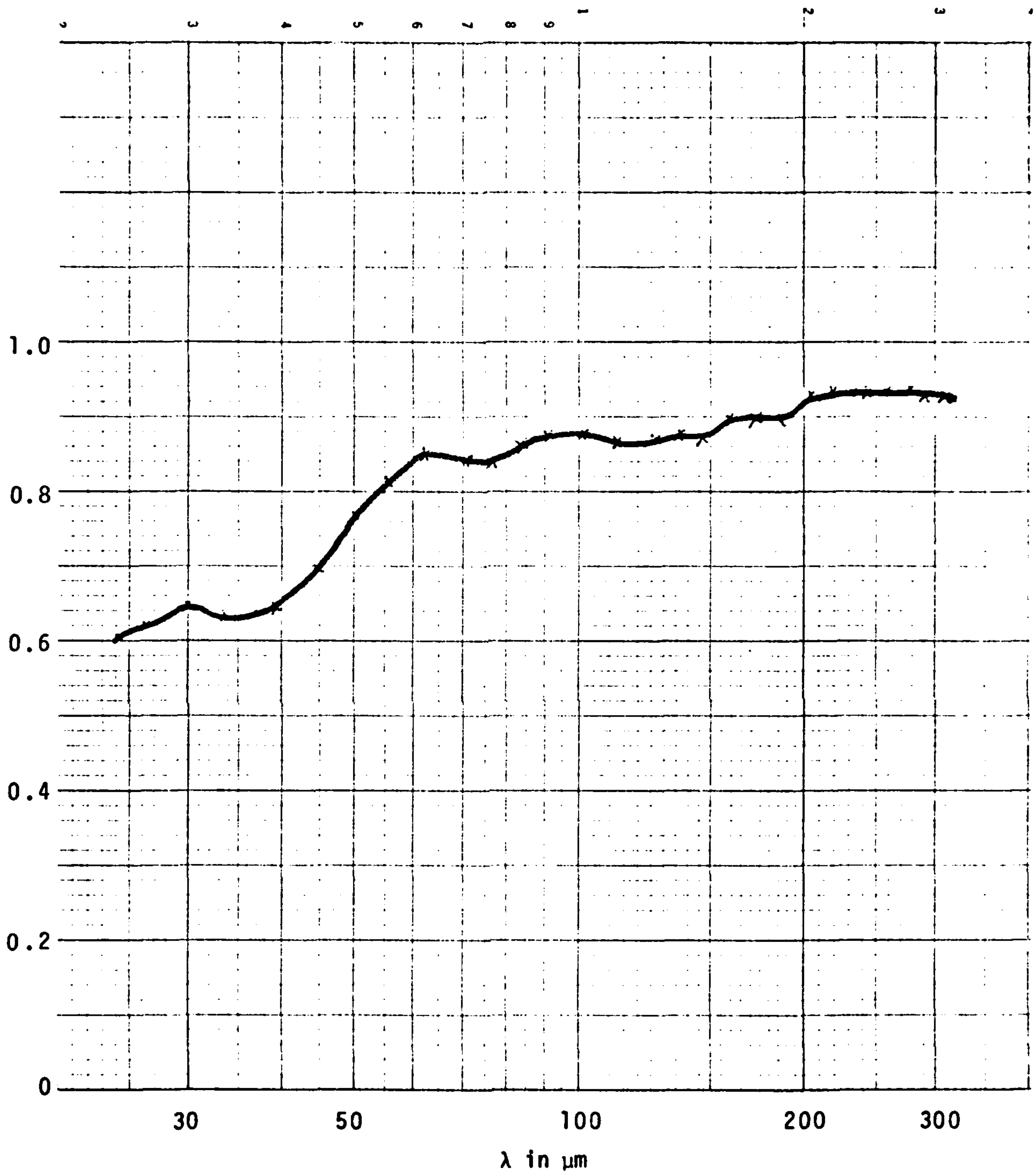

Figure 2.2-4. 1.5 mm TPX, 300°K, #600 Finish, Wedged.

2.3 ELECTRONICS

The basic interferometer scanning circuitry was a standard Block controller, which utilizes laser reference signal and the white light reference signal in a closed servo loop, maintaining scan velocity ($\dot{B}$) to better than 1% uniformity (peak-to-peak). The controller also provided the sampling signal for the computer system A/D converter, based on these reference signals.

The signal from the detector was amplified by a Model LN-6 preamplifier matched to the detector, which had a noise voltage referred to the input of less than 5.8×10^{-9} $V/Hz^{1/2}$ over the frequency range of interest. Bolometer bias was provided through a 2.5 megohm wire wound resistor mounted on the cold surface. Additional amplification of X10 was provided by a Block fabricated amplifier, designed to drive the long coaxial cables to the on-line computer system used to process the data.

A Krohn-Hite electrical filter was used at the input to the A/D to limit the noise bandwidth in the measurement. The band selected was 50 to 1000 Hz, corresponding to 100 microns to 2 millimeters, with high rejection beyond these 3 db points. As indicated before, amplitude and phase variations resulting from this filter were eliminated in the data processing.

2.4 DATA SYSTEM

All data were processed on a modified Digilab, Inc. DL-100 data system owned by Block Engineering and used for all processing of field measurement data as well as laboratory checkout and calibration of Block Fourier transform spectrometers.

This system is based on a Data General Corporation NOVA 1200 minicomputer with 32,768 words of core memory. It also includes a 12 bit, 100 kHz analog-to-digital converter, graphic scope display, video operator terminal, 512 thousand words of fixed head disk storage, digital magnetic tape unit, and digital plotter. This, together with standard Digilab software, and Block emission software package, provide a comprehensive system for processing data from Fourier transform spectrometers.

3. MEASUREMENTS

A variety of preliminary measurements were made in the check-out and testing of the equipment, and transmission measurements were made in the laboratory and outside, under varying weather conditions. All measurements were made at the Block Engineering location in Cambridge, Massachusetts, which is about 5 miles from the ocean (Massachusetts Bay) and is roughly 50 feet above sea level.

3.1 PRELIMINARY MEASUREMENTS

In addition to radiometric verification of detector sensitivity and source radiance, a number of measurements were made to optimize the beamsplitter thickness. Beamsplitters using 25, 50, and 125 micron mylar films were fabricated and tested, and 50 micron film was selected for the transmission measurements. In addition, the mercury arc lamp was compared to a standard 1200°K blackbody source and its spectral characteristics were determined.

3.2 INTERIOR MEASUREMENTS

Transmission measurements were made in the laboratory and connecting hallway, allowing a 25 meter maximum path. The transmitter and receiver were separated in these measurements, with the transmission path between in the standard two-ended technique. These measurements were performed under ambient laboratory conditions with temperatures between 19° and 21°C, and undetermined moderate relative humidities.

Alignment techniques were worked out, and the handling of the equipment, including gas and water lines was established. Alignment was greatly facilitated with the arc lamp, which provided a clear visible image to work with. After visual alignment, signal levels were determined in the interferogram output, and signal maximization was obtained through fine adjustment of the pointing.

3.3 EXTERIOR MEASUREMENTS

It was considered essential that the transmitter and receiver be protected against precipitation, and the desirability of making measurements over several different path distances precluded using the standard two-ended technique. A large flat mirror was placed on a tripod at the remote points, and the transmitter and receiver were mounted next to each other on

tripods within a garage, with the large door open. Coaxial cabling several hundred feet long provided signals to the computer system in the laboratory.

Weather data was obtained from the local office of the National Weather Bureau, recorded at Logan Airport, as it was not possible to set up a weather station at the site as we had planned. The errors in these data are probably not great, as the measurements were taken under conditions where large scale, uniform patterns prevailed over the entire Boston area, with excellent mixing from on-shore winds (SE-SW).

3.4 DATA REDUCTION

Interferograms were digitized at a sampling interval of 64X the laser wavelength, with the signal channel electrically filtered from 50 to 1000 Hz. This produces a free spectral range extending to 123.45 cm^{-1}, and optical filtering strongly rejects radiation beyond this limit. At this sampling interval, the 0.1 cm^{-1} resolution interferograms were 2048 data points long.

Successive scans from a given run were digitized and coherently added (signal averaged) to improve signal-to-noise ratio. In general, from 64 to 512 scans were averaged for each spectrum, with more scans used for low level measurements such as background determination and the longer path lengths.

Despite the fact that the interferometer was used as a modulator for the mercury arc lamp, which would eliminate any unwanted background radiation, source blocked measurements indicated measurable background signals for some measurement geometries, particularly at short range. Where this background was measurable, it was collected and subtracted from the signal interferogram.

The spectra were computed* from the interferograms by apodizing them, zero filling, and performing Fast Fourier Transform (FFT) with phase correction. The apodization function corrected for the single-sided interferogram, which extends only a short distance on one side of the zero path (centerburst) position. The truncation of the interferogram on this short side would produce considerable artifacts in the spectrum, so the apodization function increases linearly from zero through the zero path position to unity at an equal distance on the long side. The apodization function remains unity to the end of the

* For a more complete discussion of the following process see, for example, Transform Techniques in Chemistry, Edited by Peter R. Griffiths, Plenum Press.

interferogram, where signal levels have become low enough that artifact generation is insignificant due to truncation. The resulting spectra have 2048 real data points after transformation.

To compute atmospheric transmission, the spectrum measured over the desired path is simply divided by a short path, or ideally, a zero path spectrum with no atmospheric attenuation. The result is then scaled by a factor which corrects for the difference in the measurement geometries for the two spectra. Even if the short path spectrum is not at zero distance, the ratio is the transmission of the path difference between the two measurement positions, assuming constant, homogenous atmospheric conditions at all points along the paths.

In practice, the shortest practical path for this set of measurements had sufficient atmospheric attenuation in several spectral intervals to effectively block that radiation, producing nulls in the zero path spectrum. This creates a problem in using this spectrum in the denominator for the transmission ratio. Fortunately, the longer path spectrum suffers a broader "complete" attenuation in the same spectral intervals due to the increased path length. By artificially changing the zero amplitude intervals in the zero path spectrum to some positive value, we avoid the problem of dividing zero by zero and maintain the integrity of the ratio.

Due to the limited nature of this measurement program, the geometrical scale factors to convert the ratio spectra from relative to absolute transmission were not determined. It is hoped that further effort will be possible in the future, in which correction to absolute transmission will be an integral part of the program.

A number of the earlier spectra have not been ratioed to obtain relative transmission, due to the channeling effects noted earlier. These ratios, which had been expected to eliminate channeling, proved to contain residual channel effects sometimes larger than those in the spectra themselves, and we believe that ratio spectra are not reliable in these circumstances.

4. DATA

Spectral plots were made over the period from 9 November to 15 December 1978, as indicated in the data log in Table 4.0-I. The earlier measurements were involved in preliminary testing and equipment evaluation, but transmission path measurement is implicit in these data. Later measurements were solely directed at the measurement of atmospheric transmission. Data not indicated in the listing were either unsatisfactory or were directly incorporated into other data for plotting, as for background measurements of interferogram files in general.

The serial number of plotted spectra is provided by the computer system, and was not consistent from day to day, as other programs also used that system. The range indications are sketchy in the preliminary measurements, but were carefully measured for the outside transmission spectra taken during December. The note "ZPD" refers to a zero path difference measurements, and indicated measurements through the interferometer to the equivalent focal length (EFL) of the plastic lens in the preliminary measurements. In the final measurements, the "ZPD" note refers to measurements with the path reduced to a minimum with the telescopes either transmitting through the folding mirror or "head-on," see Figure 4-1. Measured ranges are between front surfaces of the telescopes in every case. The number of scans averaged to generate each spectrum are available from the tape log, and these have generally been supplied in the listing.

Temperature and relative humidity data obtained from the National Weather Bureau are indicated. This data is provided on an hourly basis, and consequently appears in discrete blocks when several spectra were obtained in a single hour. The note "LA" indicates laboratory ambient temperatures or relative humidities, and the note "P" is used to indicate a measurement with the instrument purged with dry nitrogen gas, contained within two large plastic bags.

Data annotated here are abbreviated, but indicate the general scenario. A parameter such as frequency range, spectral resolution, beamsplitter thickness, etc. is generally retained in all following spectra at the value noted, unless another note is given. The term "HgL" refers to one of two high pressure mercury arc lamps of identical configuration that were used.

Tabel 4-Ia. Data Log

DATE	SPECTRA	RANGE	SCANS	TEMP	R.H.	DATA IDENTIFICATION
11/9	HF133	ZPD	256	LA	LA	Bolometer with heat stick
	134	ZPD	512	LA	LA	Bolometer, 20-600 Hz blackbody
	135	Unk	512	LA	LA	0.25 cm^{-1}, 40-600 Hz
	136	42"	256	LA	LA	125μm B/S, 20-600 Hz
	137	42"	256	LA	LA	0.5 cm^{-1}, 20-600 Hz
11/13	HF131	Unk	100	LA	LA	Hg Lamp, 25-600 Hz, 0.1 cm^{-1}
	132	Unk	100	LA	LA	Same, triangular apodization
	133	Unk	100	LA	LA	5-600 Hz, triangular apodization
	139	Unk	100	LA	LA	Same as 131
	140	Unk	128	LA	LA	40-1000 Hz
11/15	HF0	42"	Unk	LA	LA	HgL, 0.1 cm^{-1}, 125μm B/S, 40-1 kHz
	02	42"	Unk	LA	LA	HgL, 125μm B/S, 20-500 Hz
	03	42"	Unk	LA	LA	Same, no elect. filter
	04	42"	Unk	LA	LA	0.25 cm^{-1}, damped vibration
	05	Unk	Unk	LA	LA	Same, modified damping
	06	Unk	Unk	LA	LA	HgL-Bkgd, same, damping
	07	Unk	100	LA	LA	HgL-Bkgd, no damping
	08	42"	100	LA	LA	HgL for HF7
	09	-	100	LA	LA	Bkgd for HF7
	11	Unk	100	LA	LA	HgL for HF6
	12	-	100	LA	LA	Bkgd for HF6

Table 4-Ib. Data Log (Continued)

DATE	SPECTRA	RANGE	SCANS	TEMP	R.H.	DATA IDENTIFICATION
11/16	HF09	33"	100	LA	LA	HgL, 50 μm B/S, 50-1000 Hz
	10	33"	256	LA	LA	Same
	11	80"	256	LA	LA	Same
11/17	HF12	ZPD	200	LA	LA	Bolometer at EFL of lens
	13	ZPD	200	LA	P	Same, Purge No. 1
	14	ZPD	200	LA	P	Same, Purge No. 2
	15	ZPD	200	LA	P	Same, Purge No. 3
	16	ZPD	200	LA	P	Same, Purge No. 4
	17	ZPD	200	LA	P	Same, Purge No. 5
	18	ZPD	200	LA	P	Same, Purge No. 6
	19	ZPD	200	LA	P	Outer purge bag removed
	20	ZPD	200	LA	P	Same, some time elapsed
	21	ZPD	200	LA	LA	Inner purge bag removed
	22	ZPD	-	LA	LA	Ratio, HF21/HF20
	23	Unk	256	LA	LA	Hot resistive blackbody, 0.25 cm^{-1}
11/20	-	Unk	Unk	LA	P	HgL, 0.1 cm^{-1}, partial purge
	26	Unk	Unk	LA	P	Same, 25 μm B/S
	27	Unk	Unk	LA	P	Same
	30	Unk	Unk	LA	LA	Interferogram, 50 μm B/S, short
	31	Unk	Unk	LA	LA	Interferogram, same, long
	34	Unk	Unk	LA	LA	HgL, 0.1 cm^{-1}, 50 μm B/S

Table 4-Ic. Data Log (Continued)

DATE	SPECTRA	RANGE	SCANS	TEMP	R.H.	DATA IDENTIFICATION
Unk	HF135	33"	Unk	LA	LA	Reference for fudging
	137	80'	Unk	LA	LA	Relative transmission ratio
	138	33"	Unk	LA	LA	Fudged reference
	139	80'	Unk	LA	LA	HgL spectrum for HF137
12/4	HF 91	25M	Unk	59F	97%	HgL
	92	ZPD	Unk	59F	97%	Fudged reference
	134	ZPD	64	59F	97%	Reference head-on, F(39)
	137	50M	256	60F	97%	HgL, F(43)
	138	25M	128	60F	97%	HgL, F(45)
	139	12.5M	128	60F	97%	HgL, F(47)
	140	ZPD	64	61F	90%	HgL, F(49)
	141	100M	2 x 512	61F	90%	HgL, F(51 + 52)
	142	ZPD	64	59F	97%	HgL, head-on, F(40)
	143	ZPD	256	59F	97%	Bkgd, head-on, F(42)
	146	50M	-	-	-	Ratio, F43/F49, norm.
	147	25M	-	-	-	Ratio, F45/F49, norm.
	149	12.5M	-	-	-	Ratio, F47/F49, norm.

Table 4-Id. Data Log (Concluded)

DATE	SPECTRA	RANGE	SCANS	TEMP	R.H.	DATA IDENTIFICATION
12/5	HF134	100M	2 x 512	4C	39%	HgL
	135	50M	512	4C	39%	HgL
	136	25M	256	3C	46%	HgL
	136a	12.5M	64	3C	46%	HgL
	137	ZPD	32	2C	50%	HgL
	139	25M	-	-	-	Ratio, HF136/HF137, norm.
	141	50M	-	-	-	Ratio, HF135/HF137, norm.
	142	12.5M	-	-	-	Ratio, HF136a/HF137, norm.
	146*	50M	-	-	-	Ratio, 97%/39%
12/15	HF134	ZPD	256	3C	50%	HgL, wedged filters
	135	12.5M	256	3C	50%	HgL
	136	25M	256	3C	46%	HgL
	138	50M	512	4C	39%	HgL
	139	100M	2 x 512	4C	39%	HgL
	VF142	100M	-	-	-	Ratio, HF139/HF134
	143	50M	-	-	-	Ratio, HF138/HF134
	144	25M	-	-	-	Ratio, HF136/HF134
	145	12.5M	-	-	-	Ratio, HF135/HF134

* Ratio between data taken 12/4 and 12/5, at 50M range.

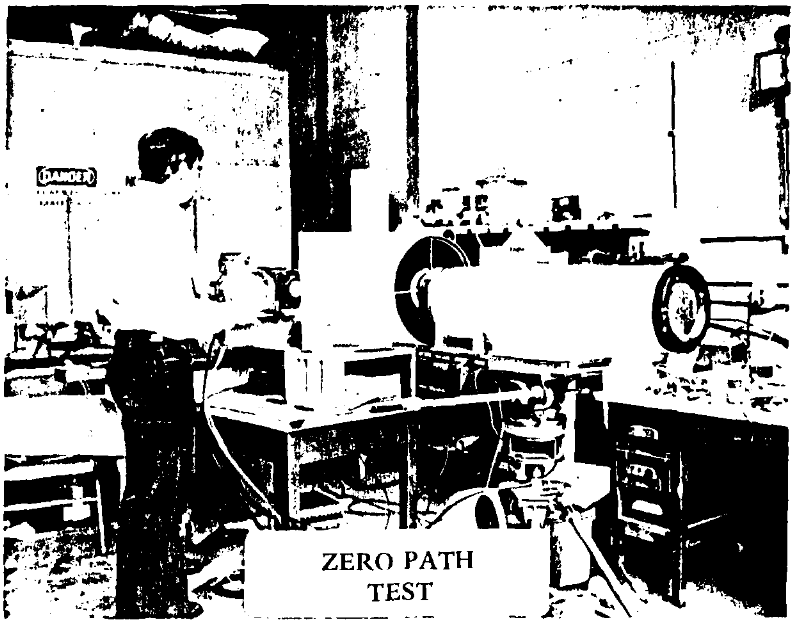

Figure 4.0-1. Zero Path Setup, Transmitter and Receiver Head-on.

As indicated earlier, the final measurements were generally taken over a folded path, unless specifically noted. In some cases, the original data files are noted; e.g. F(39) is the interferogram for HF134.

The barometric pressure on 4 December was 29.3 inches of mercury, and the wind was from 17 to 23 mph, gusting to about 30 mph from the soutwest. The pressure on 5 December was 29.7 inches of mercury, and on 15 December was 29.9 inches of mercury. The wind velocity was not recorded, but was generally from the southeast on these days. The sky on all three days was partly cloudy and the visibility was moderately good, perhaps averaging 10 miles.

4.1 SPECTRA

Selected spectra are presented which document the transmission measurements fully, but avoid much extraneous material. All data taken during this program are available on computer tape stored at Block Engineering, Inc.

Figures 4.1-1, 4.1-2, and 4.1-3 show preliminary measurements of the Philips mercury arc lamp source with 25, 50, and 125 micron mylar beamsplitters, respectively. Figures 4.1-1 and 4.1-3 show some artifacts in the region below 10 cm^{-1}. The measurement of the background modulated by the interferometer, shown in Figure 4.1-4, also contains the artifacts, which disappear when the background is subtracted in Figure 4.1-5. The effects of channeling are especially significant in Figure 4.1-2, and appear to some extent in all spectra taken before 15 December, when the wedged filters were installed.

A typical interferogram is shown in part in Figure 4.1-6, obtained at essentially zero path difference with the mercury lamp source. A slight assymetry is common in most interferograms, and the phase shifting which produces this is accurately corrected in the data processing used by Block. The raw spectrum obtained is represented by Figure 4.1-7, which shows a measurement at 25 meters range. To obtain the relative transmission, this spectrum would be ratioed with a reference spectrum taken at zero path difference. In order to avoid division by zero in the computation, the reference spectrum is "fudged," as shown in Figure 4.1-8.

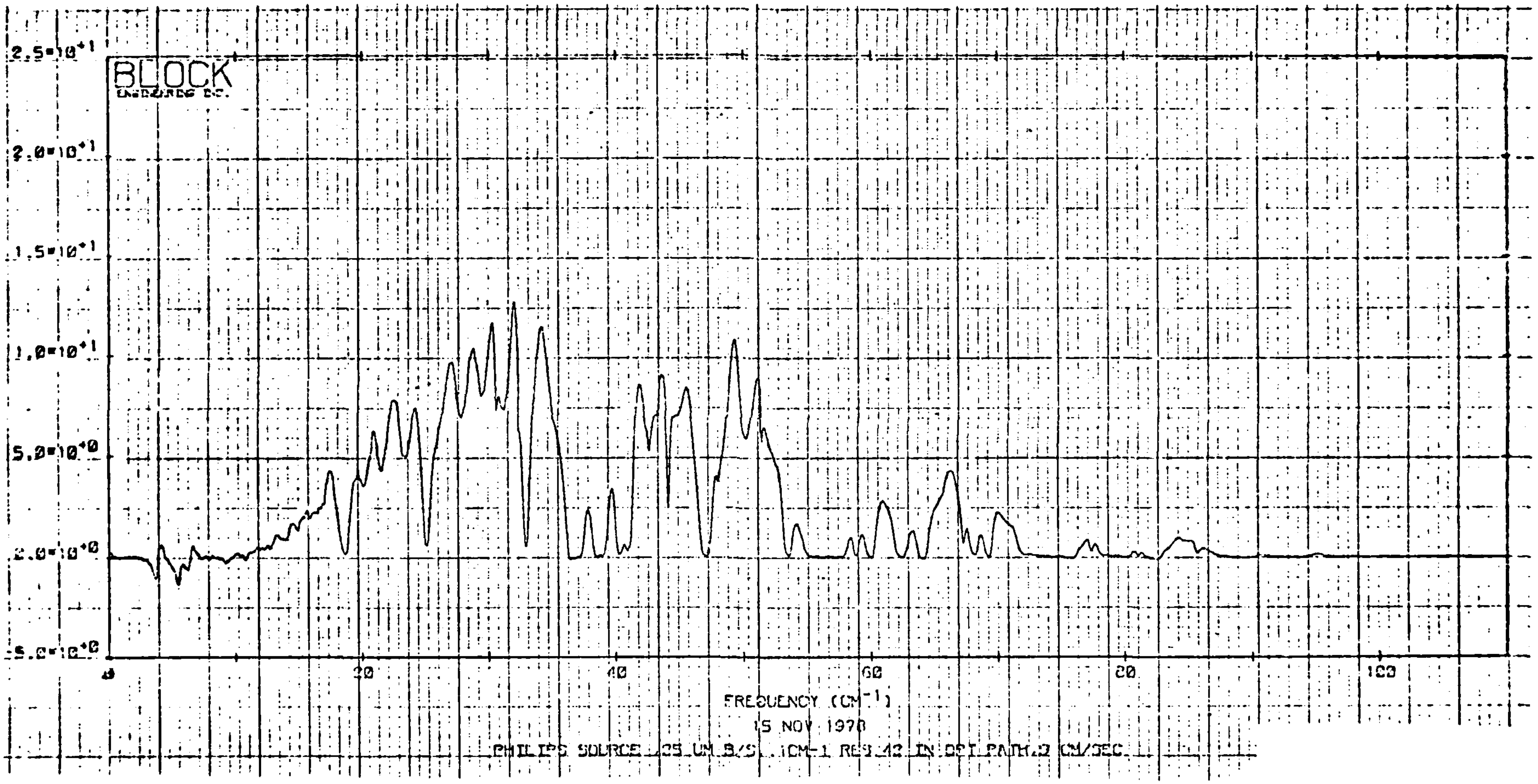

Figure 4.1-1. Arc Lamp Spectrum with 25 Micron Beamsplitter.

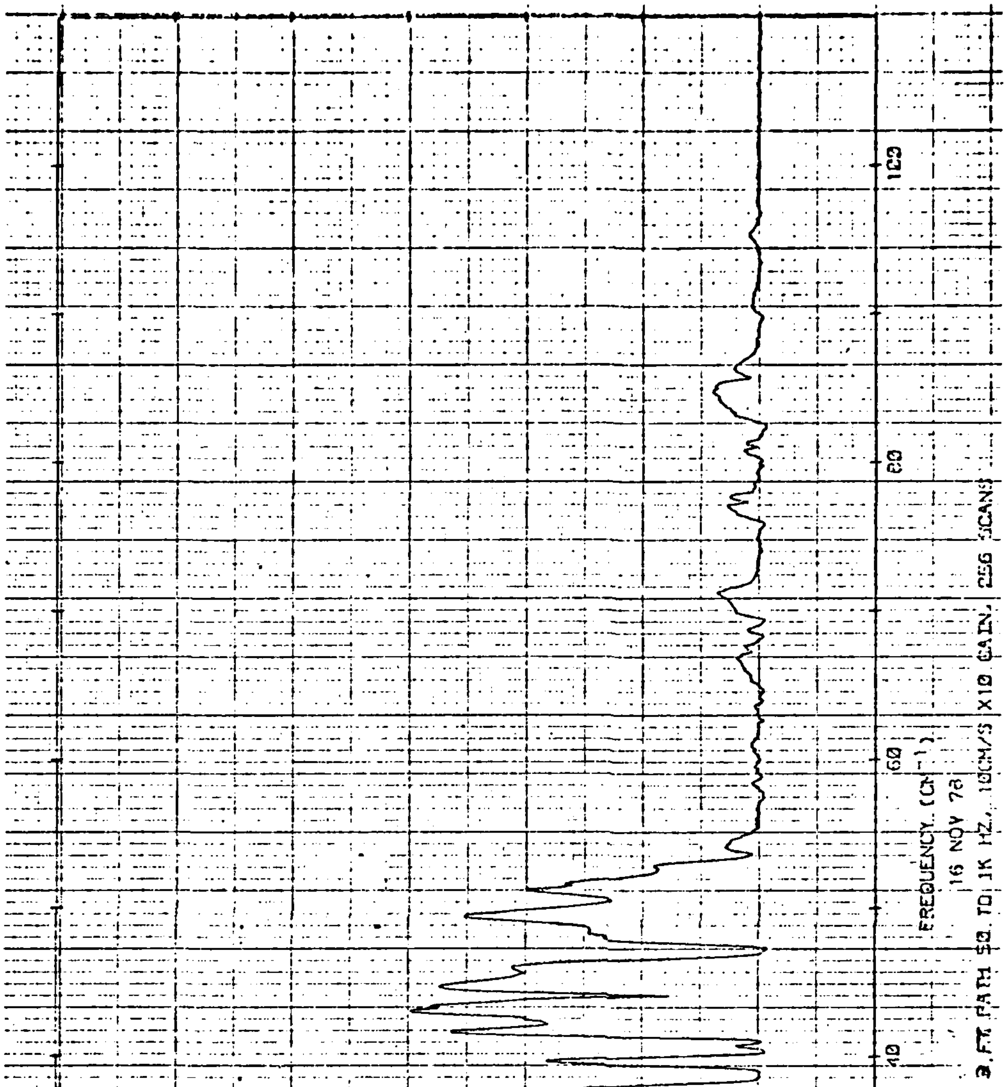

Figure 4.1-2. Arc Lamp Spectrum with 50 micron Beamsplitter.

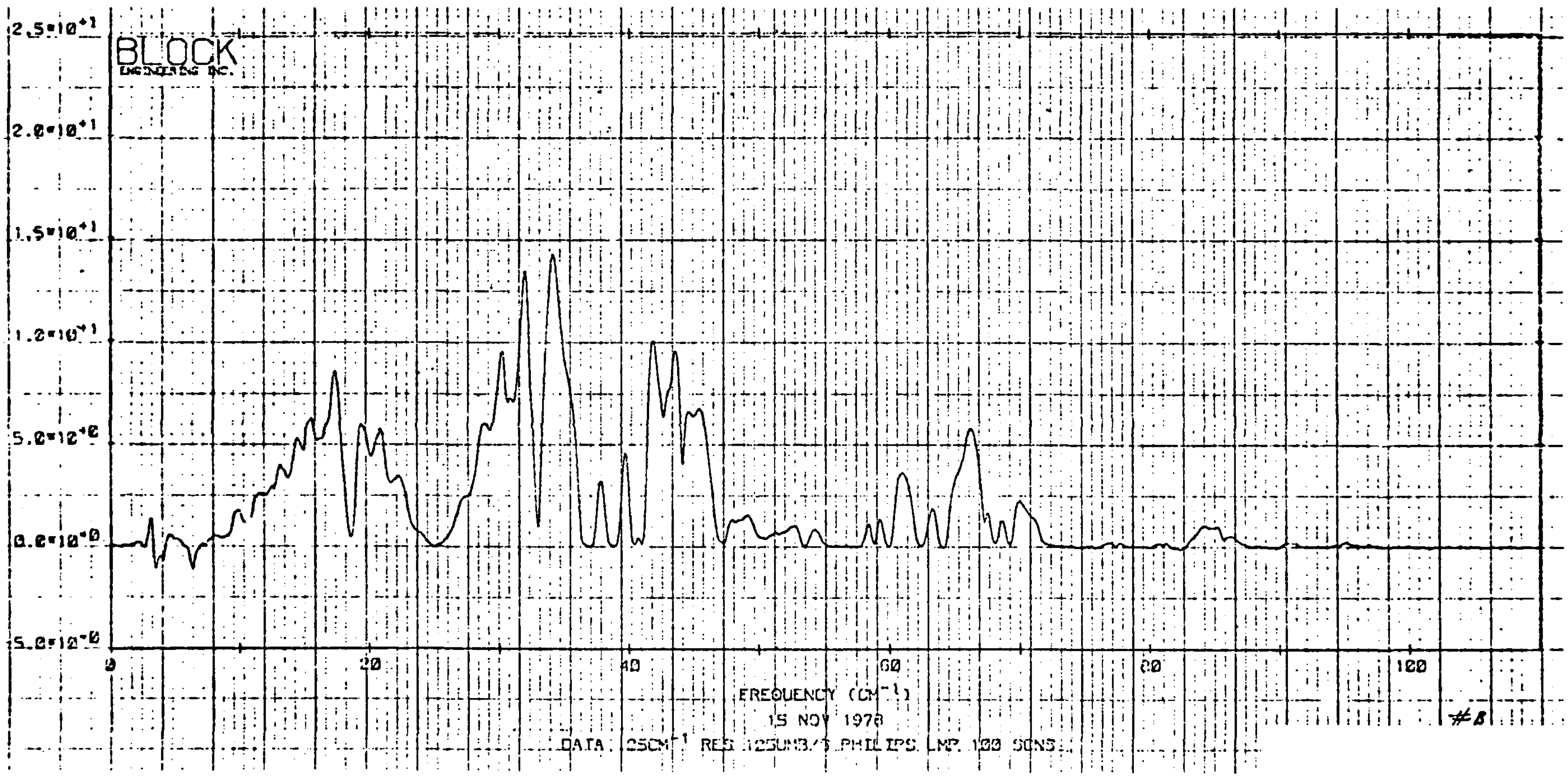

Figure 4.1-3. Arc Lamp Spectrum with 125 Micron Beamsplitter.

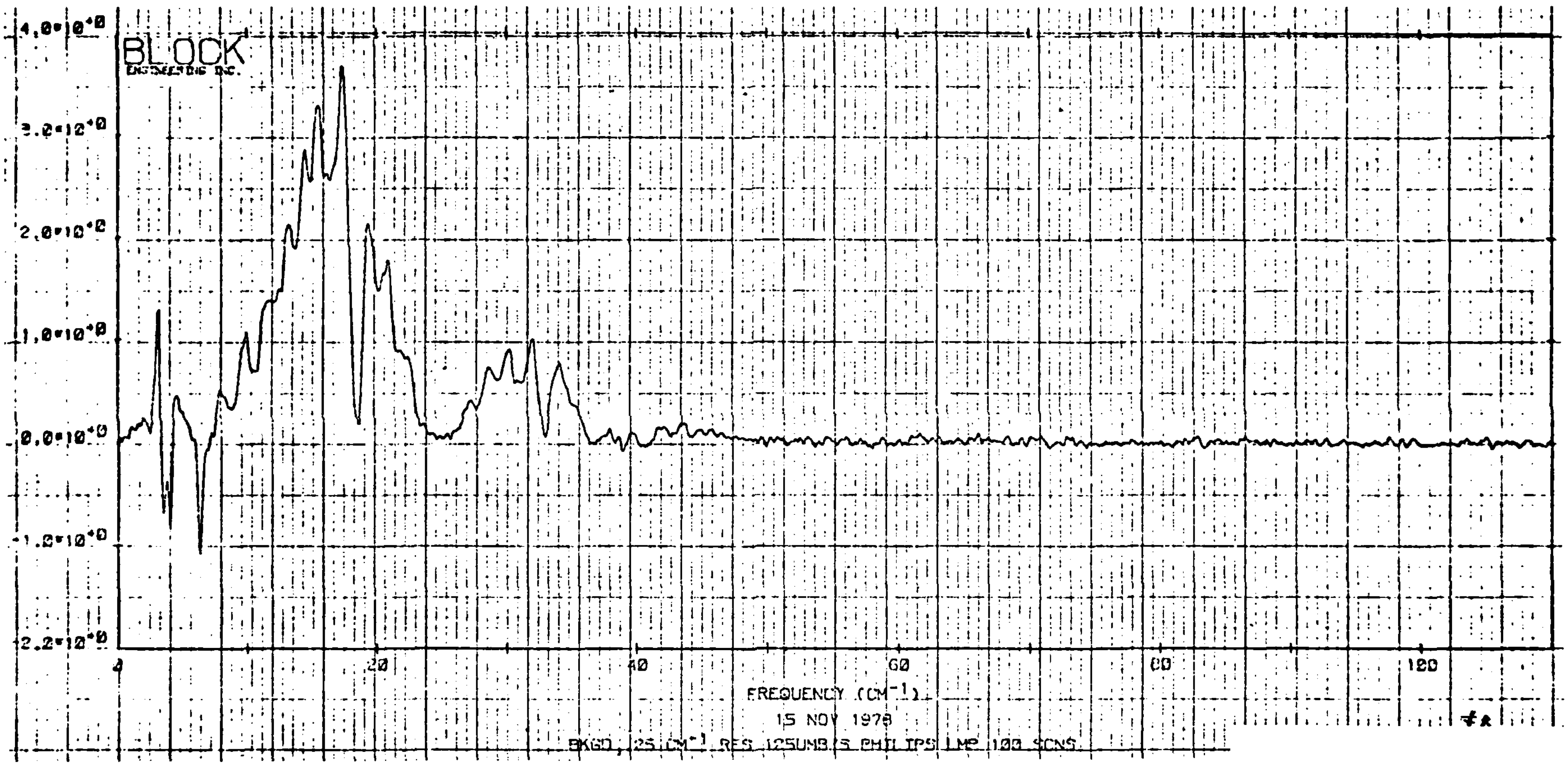

Figure 4.1-4. Background Spectrum with 125 Micron Beamsplitter.

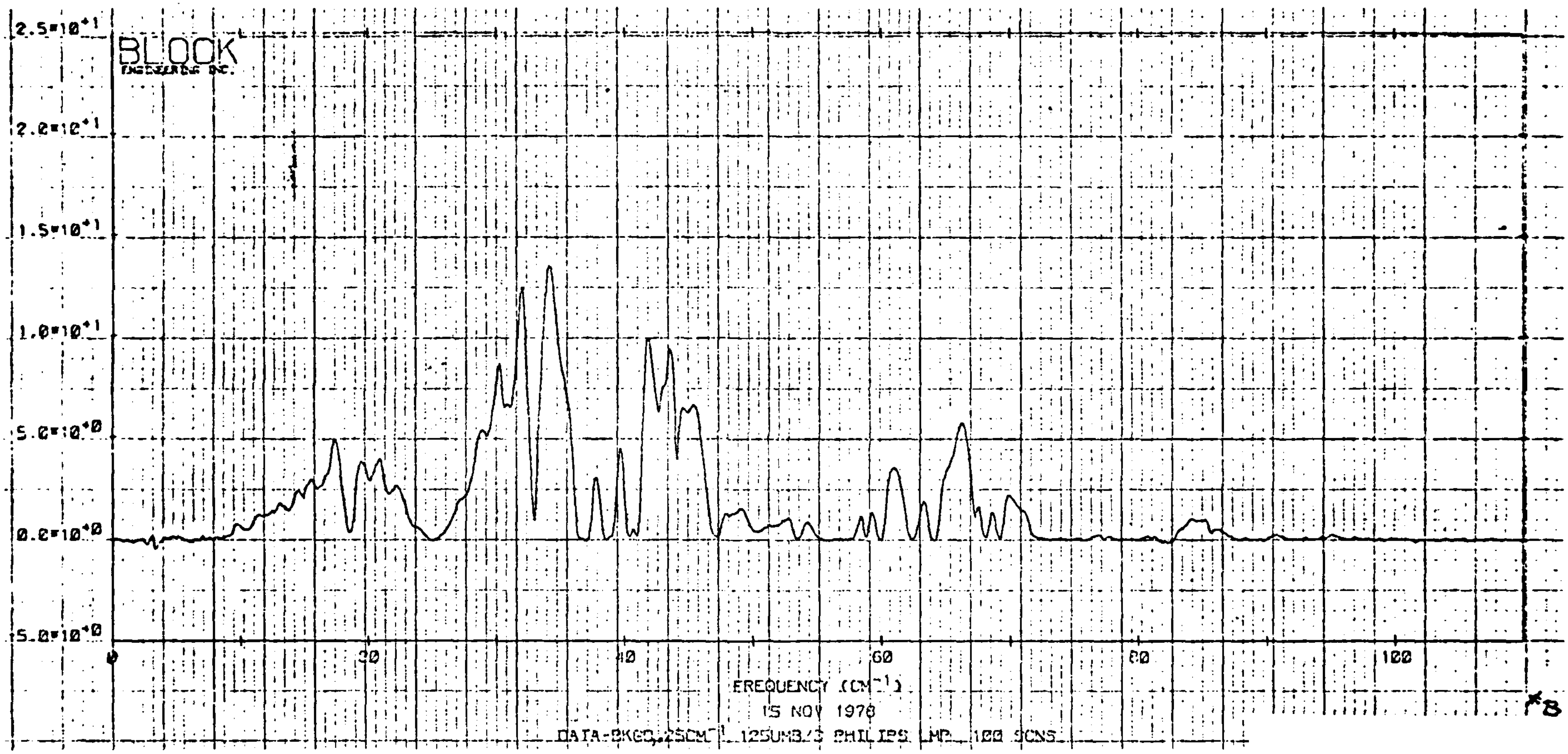

Figure 4.1-5. Arc Lamp Spectrum with Background Spectrum Subtracted.

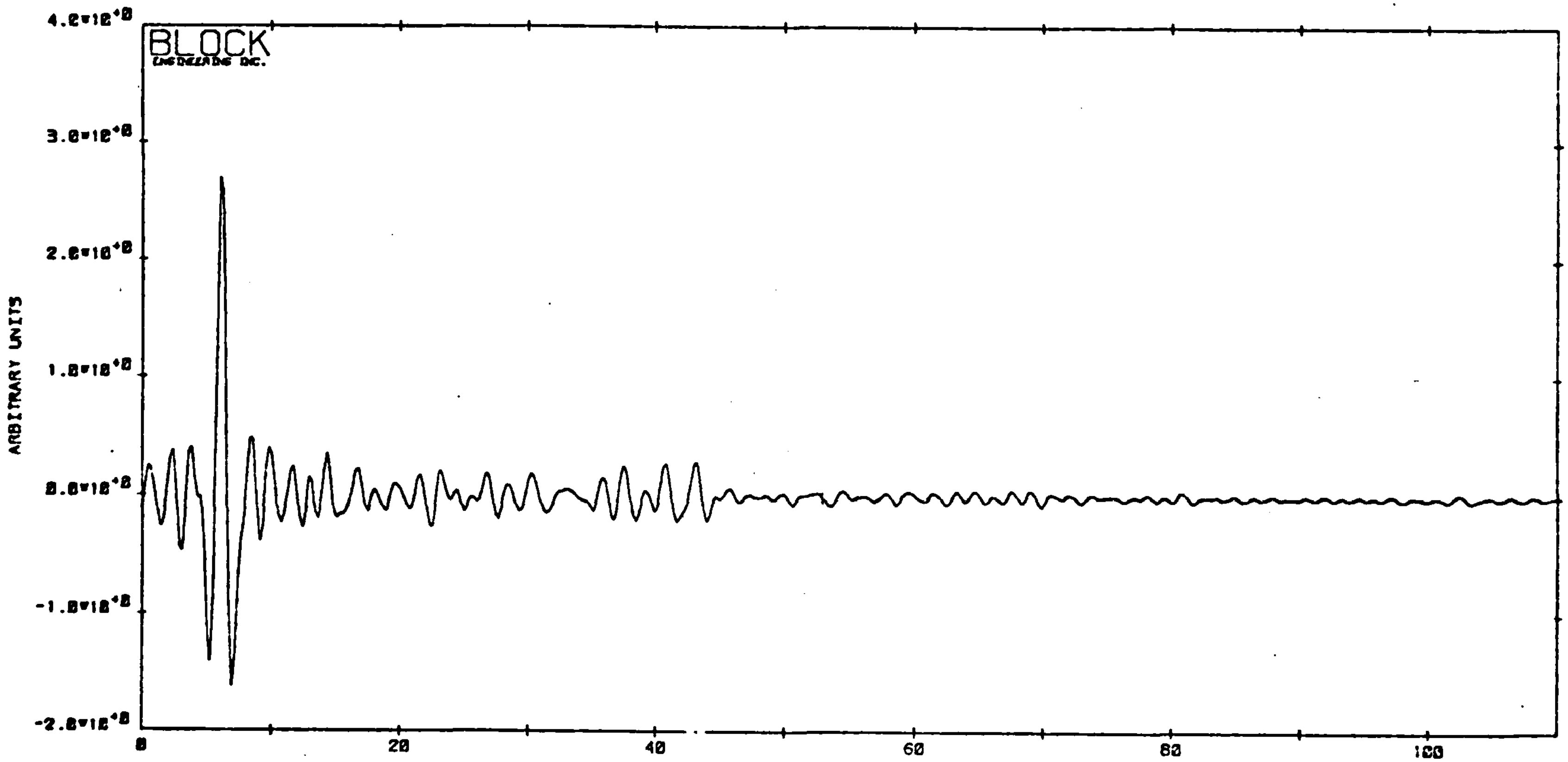

20 NOVEMBER 1978

IL 3MM GE BOLOMETER ,TYPICAL INTERFEROGRAM ,50 UM B/S

MF 31

Figure 4.1-6. Arc Lamp Interferogram.

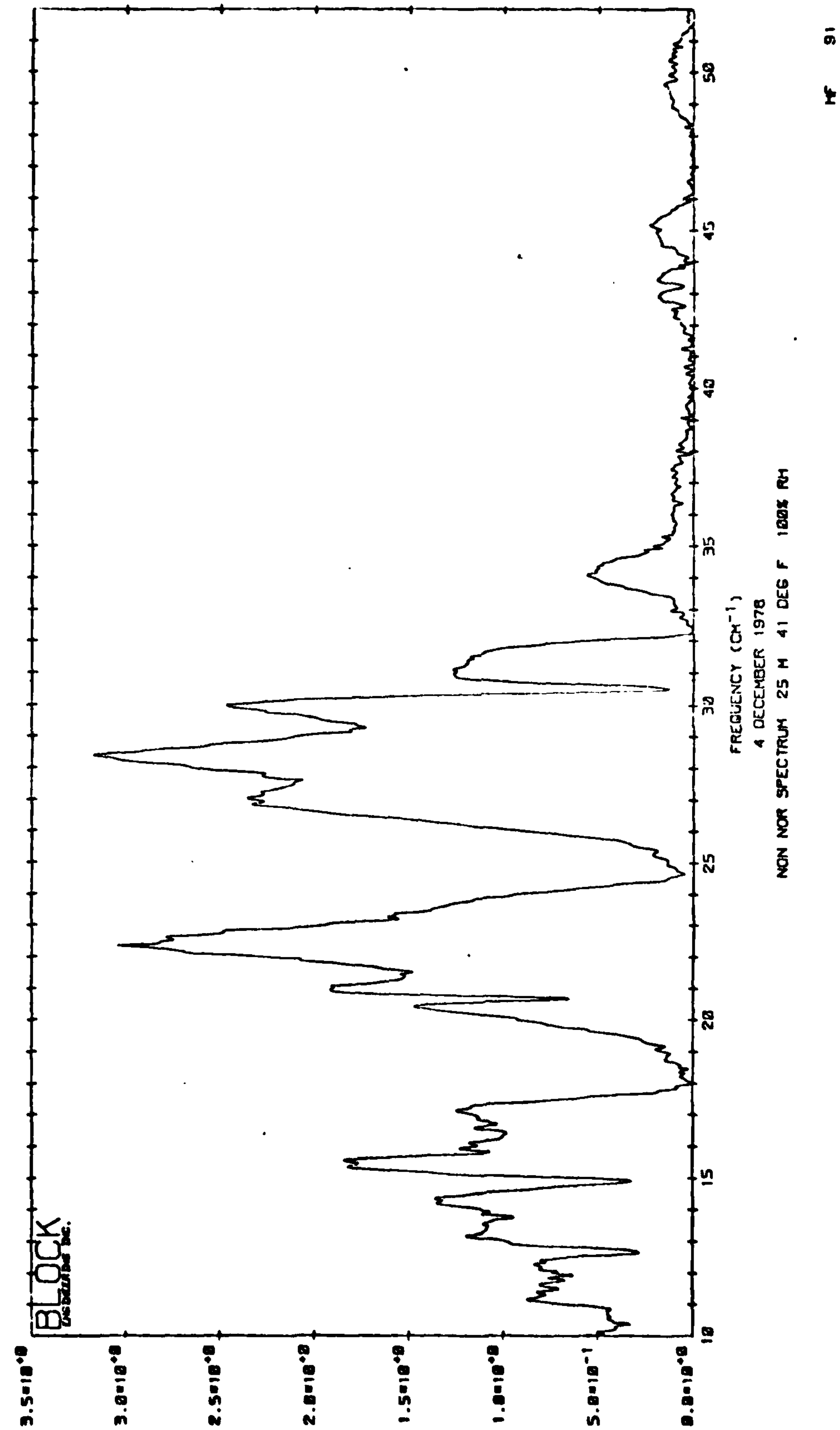

Figure 4.1-7. Non-Normalized Spectrum.

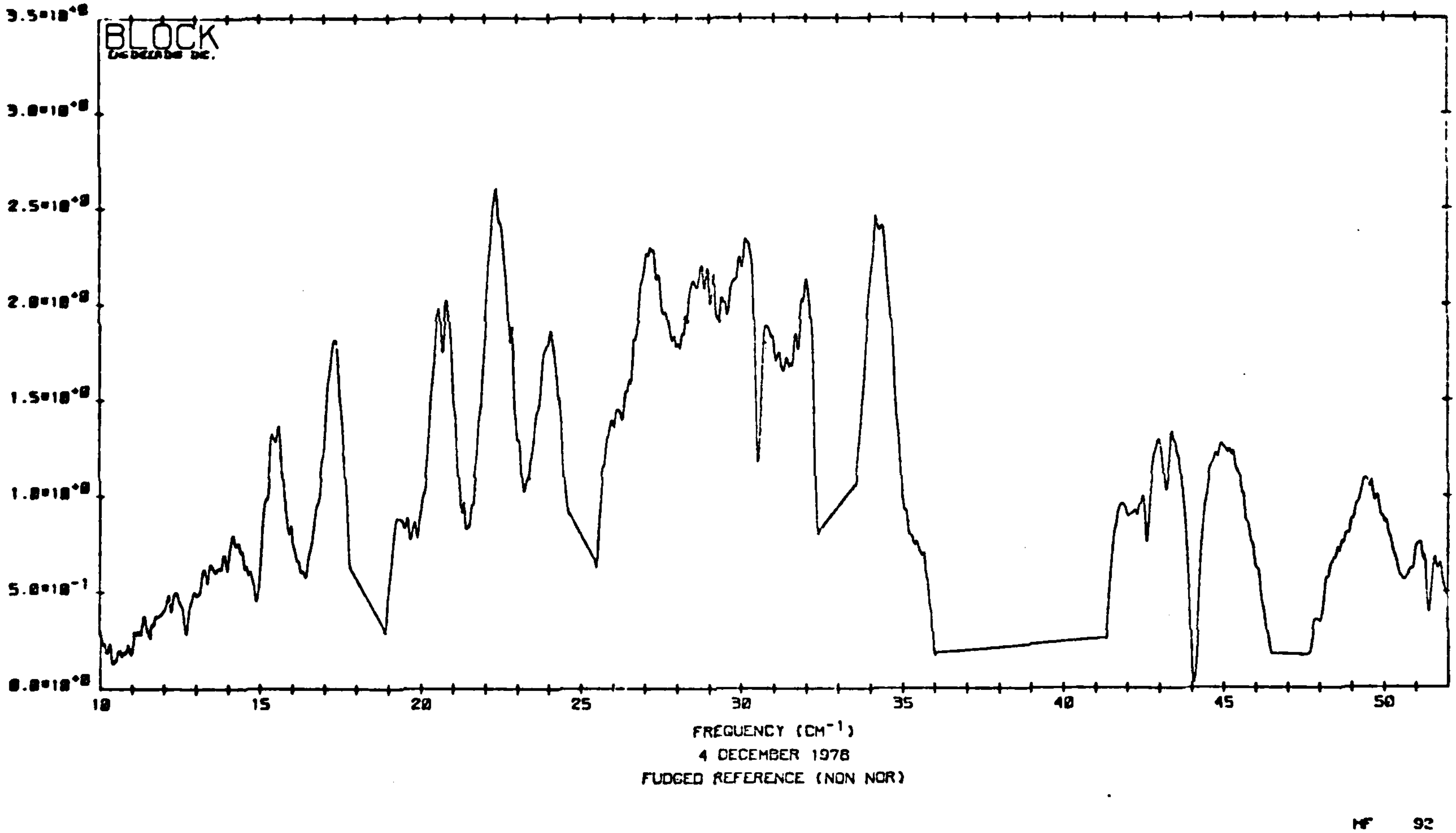

Figure 4.1-8. Fudged Reference Spectrum.

Figures 4.1-9, 4.1-10 and 4.1-11 show the data obtained at effective zero path with 90-97% relative humidity. The first two spectra show the arc lamp present and then off, with only background present. The third shows the arc lamp present viewed by the receiver through the folding mirror, set just in front of the transmitter and receiver apertures. In either zero path measurement technique, the transfer of energy is complicated because of the different transmitter and receiver apertures, preventing an accurate determination of optical efficiency. As a result of this and other factors, we have not attempted to make absolute calibrations in this program.

The sequence of data obtained at 90-97% relative humidity are shown in Figure 4.1-12 (12.5 meters), 4.1-13 (25 meters), 4.1-14 (50 meters), and 4.1-15 (100 meters).

A similar set of spectra were obtained at 39-50% relative humidity, as can be seen in Figure 4.1-16 (zero path), 4.1-17 (12.5 meters), 4.1-18 (25 meters), 4.1-19 (50 meters), and 4.1-20 (100 meters).

Although ratioing was attempted for these spectra, the effects of channeling were so severe in the reference spectra that the ratios were seriously compromised. These ratio spectra have not been included here to avoid misleading the reader.

The final set of data, shown in Figures 4.1-21 (zero path), 4.1-22 (12.5 meters), 4.1-23 (25 meters), 4.1-24 (50 meters), and 4.1-25 (100 meters), were obtained with relative humidity of 39-50%. The elimination of channeling effects can be seen resulting from the wedged filters installed.

Ratio spectra have been computed for these data, and can be seen in Figure 4.1-26 (12.5 meters), 4.1-27 (25 meters), 4.1-28 (50 meters) and 4.1-29 (100 meters). These ratio spectra have not been converted to absolute transmission, and the computational spectral range was limited to 10 to 55 cm^{-1}, which somewhat limits the utility of the data. The only technique which could have given an approximation to absolute transmission in the short time remaining was the use of estimated extinction parameters in clear (?) bands, and the computed adjustment for each path length. This approach would be seriously in error if anomalous absorptions were present, as was quite possible. The spectral range limitation was based primarily on the low signal levels below 10 cm^{-1} and above 55 cm^{-1}, which give excessive and unreliable noise variations there.

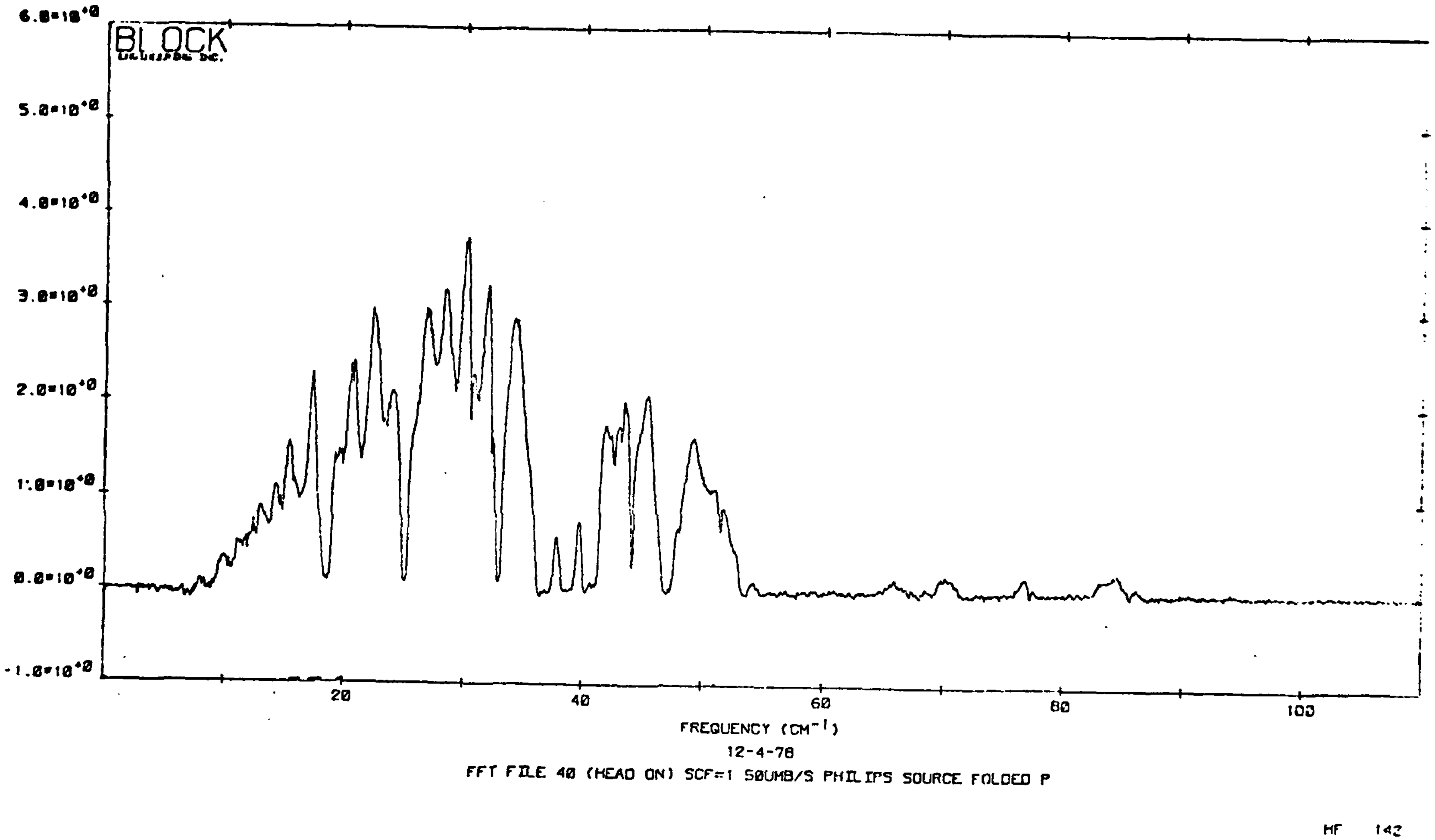

Figure 4.1-9. Zero Path (Head-on) Spectrum, 97% R.H., 15°C.

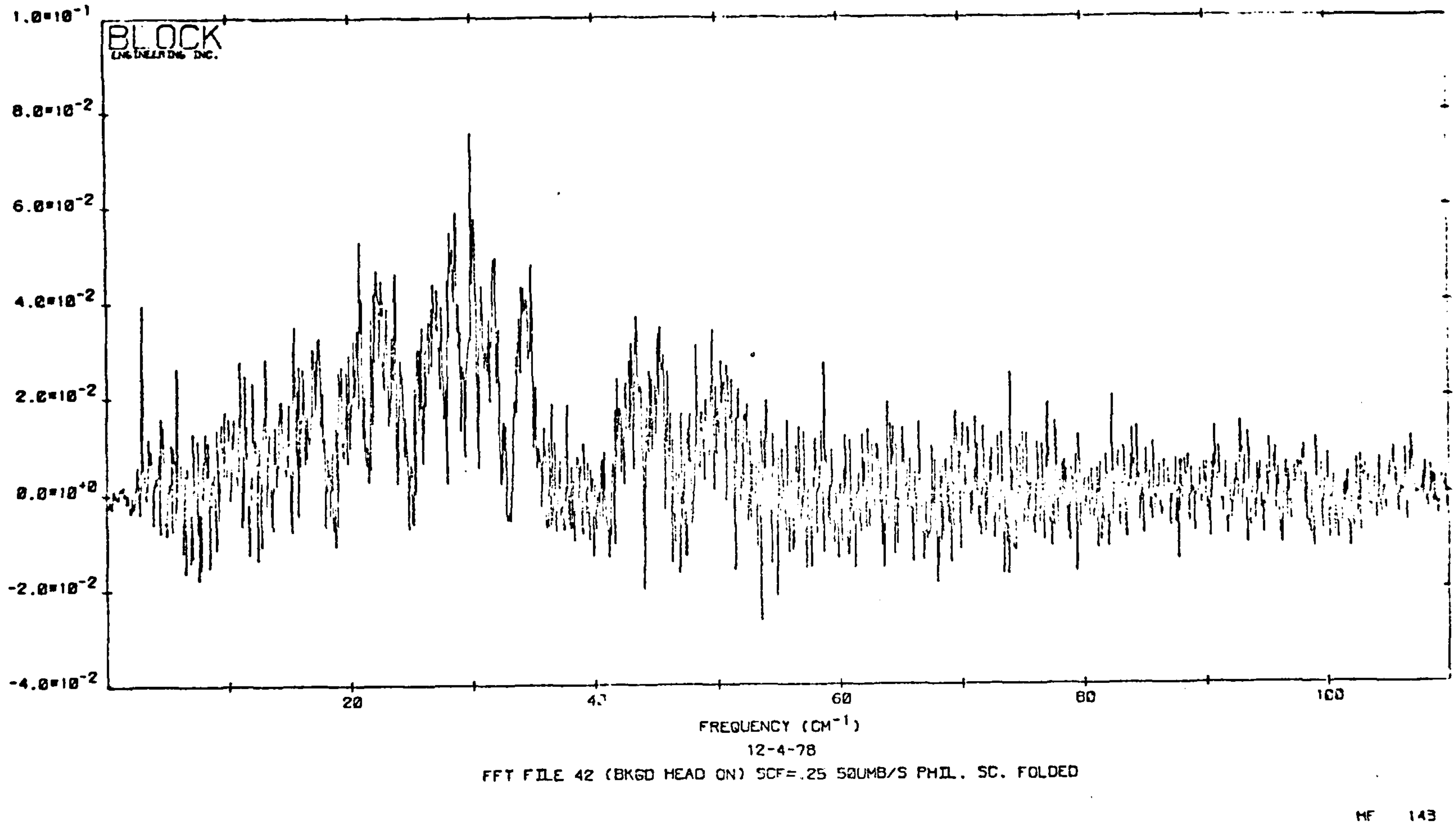

Figure 4.1-10. Background (with mirror) Spectrum, 97% R.H., 15°C.

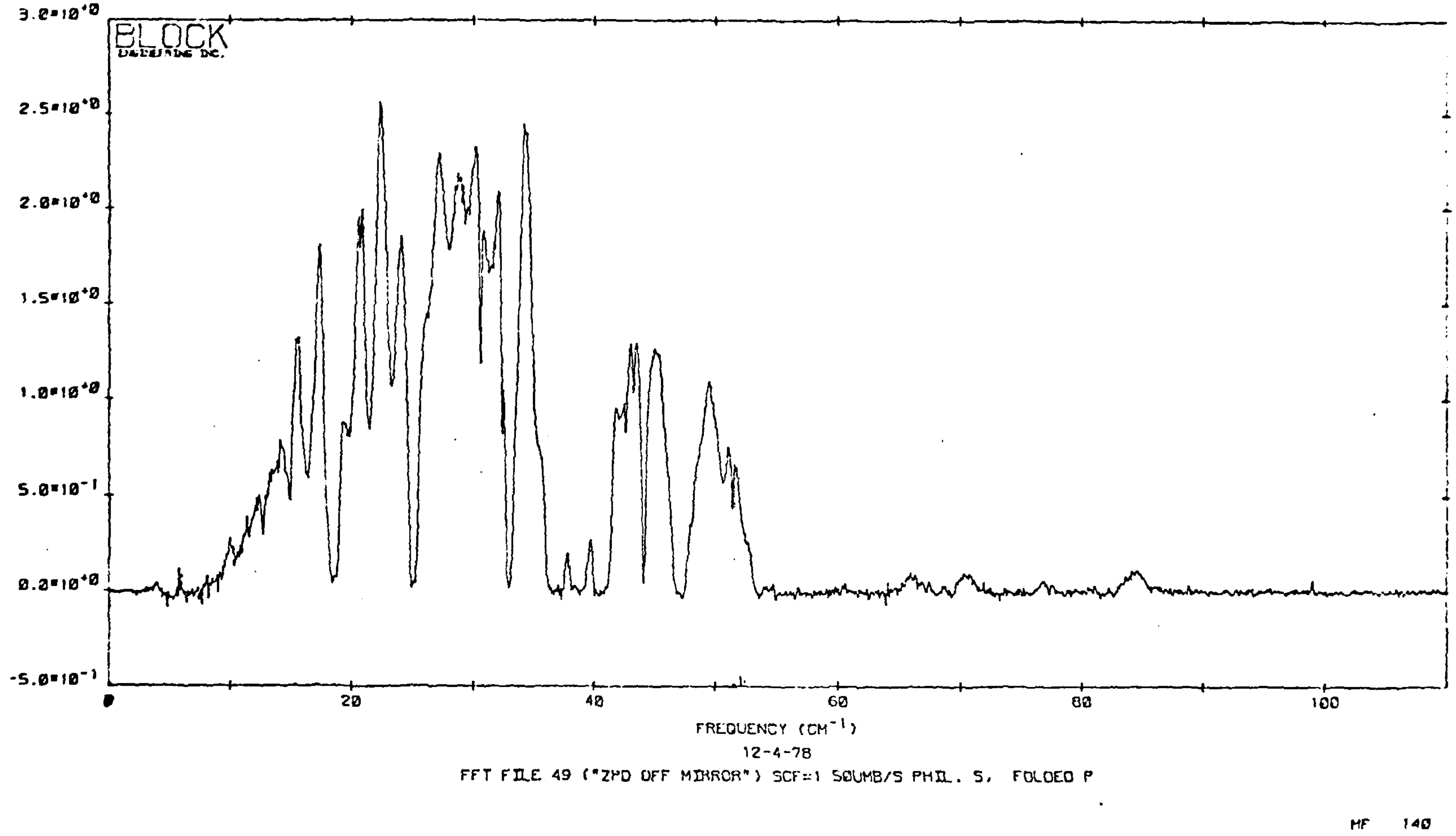

Figure 4.1-11. Zero Path (Folded) Spectrum, 90% R.H., 16°C.

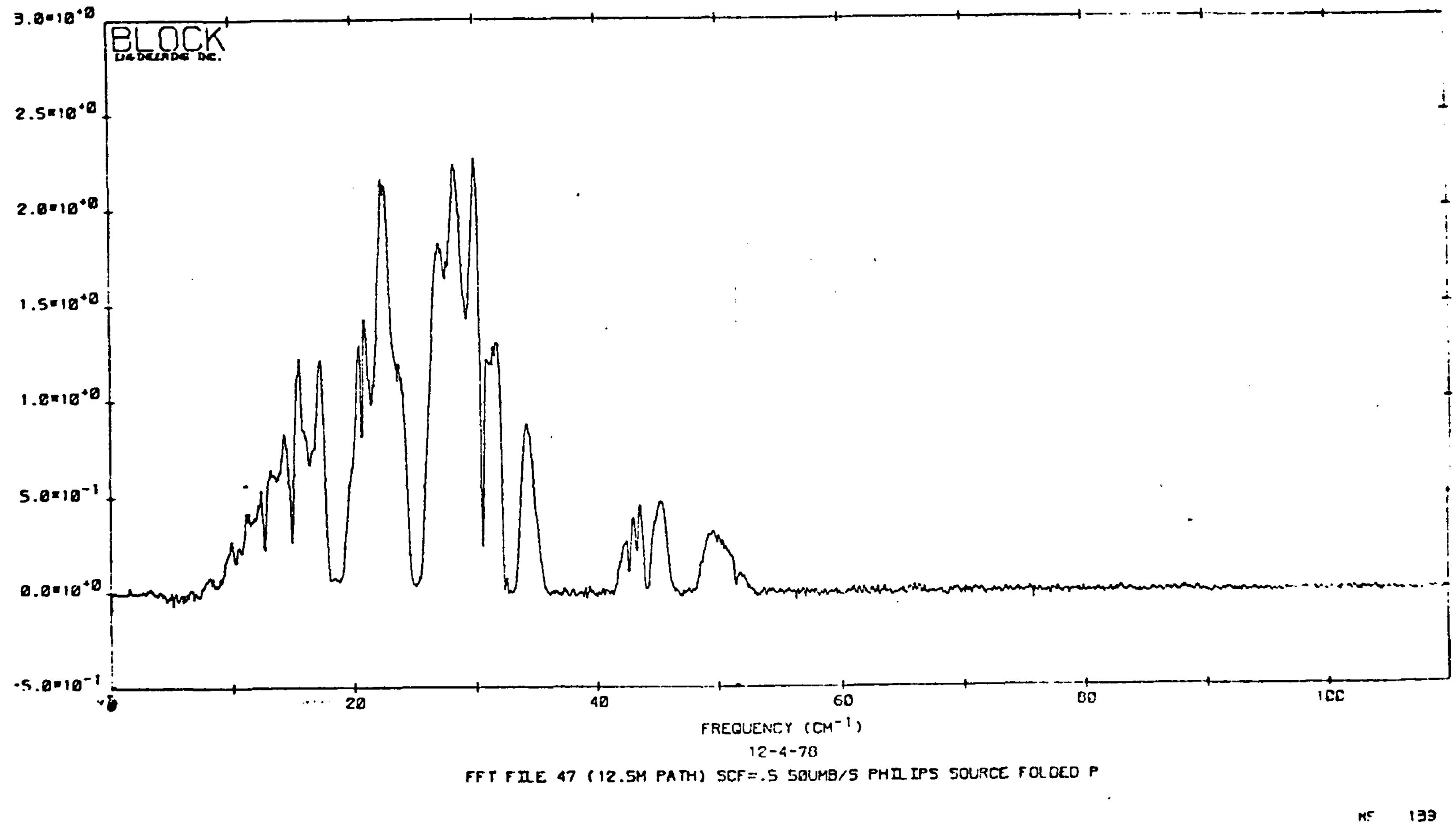

Figure 4.1-12. 12.5 Meter Spectrum, 97% R.H., 16°C.

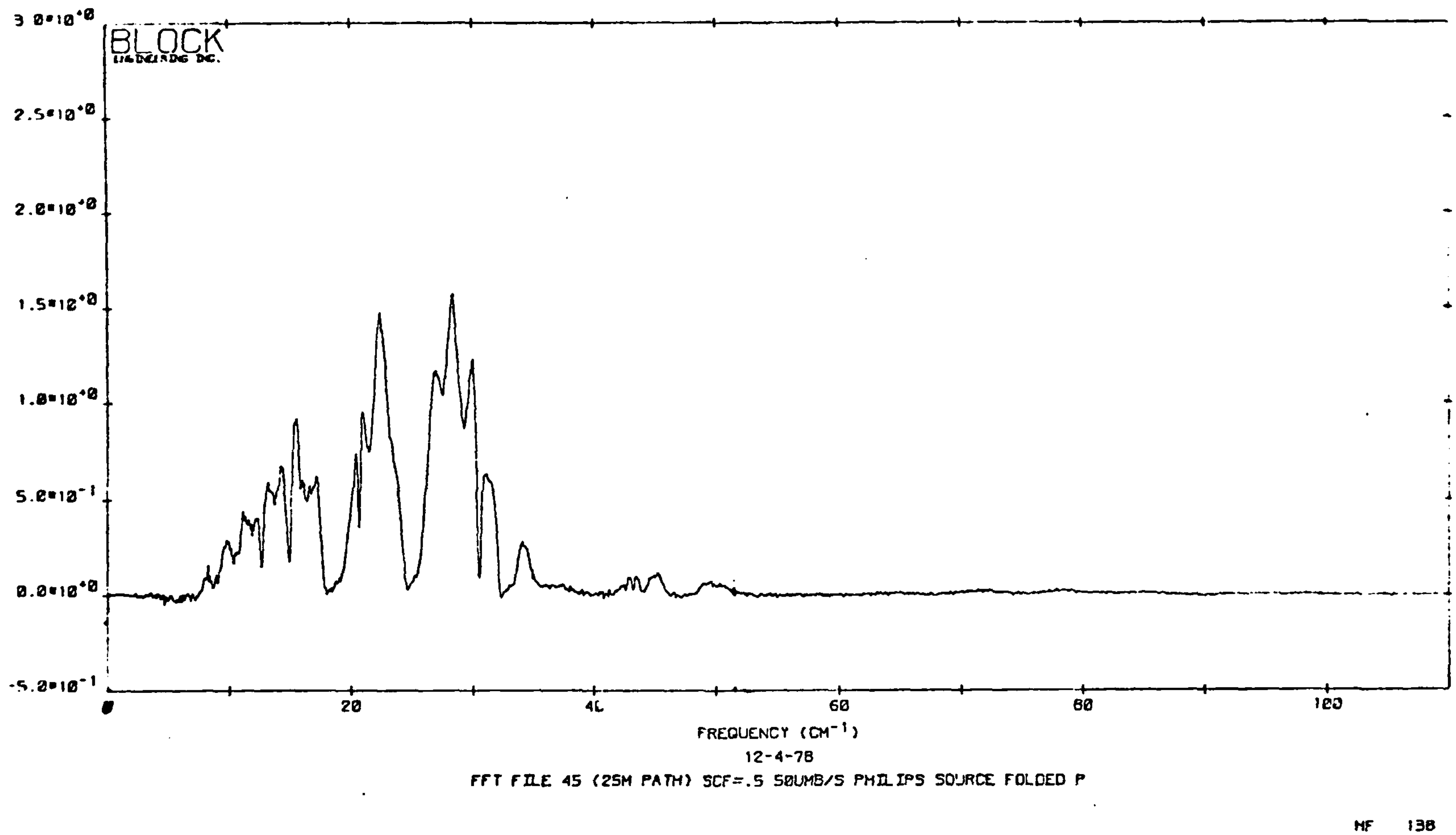

Figure 4.1-13. 25 Meter Spectrum, 97% R.H., 16°C.

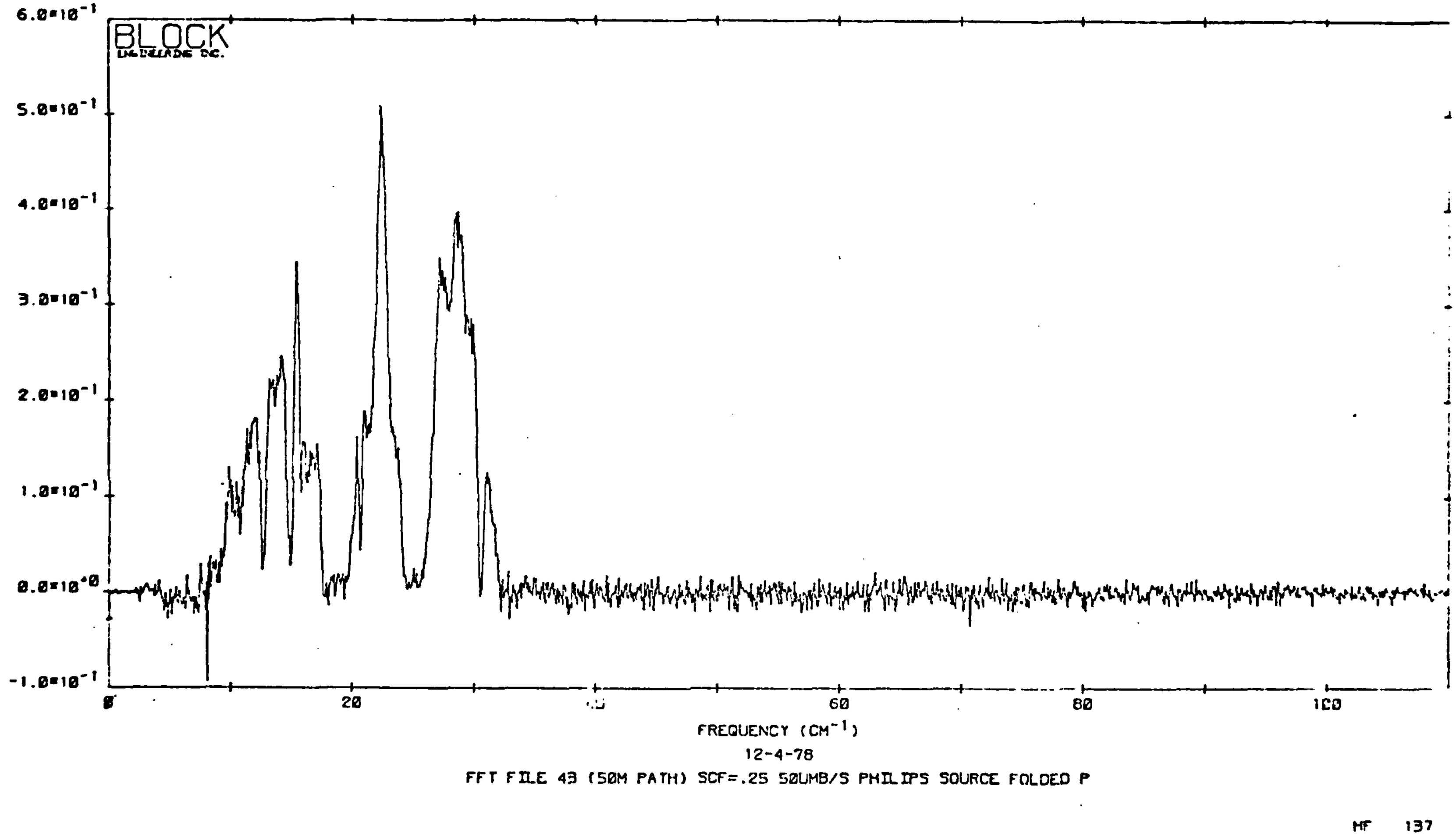

Figure 4.1-14. 50 Meter Spectrum,
97% R.H., 16°C.

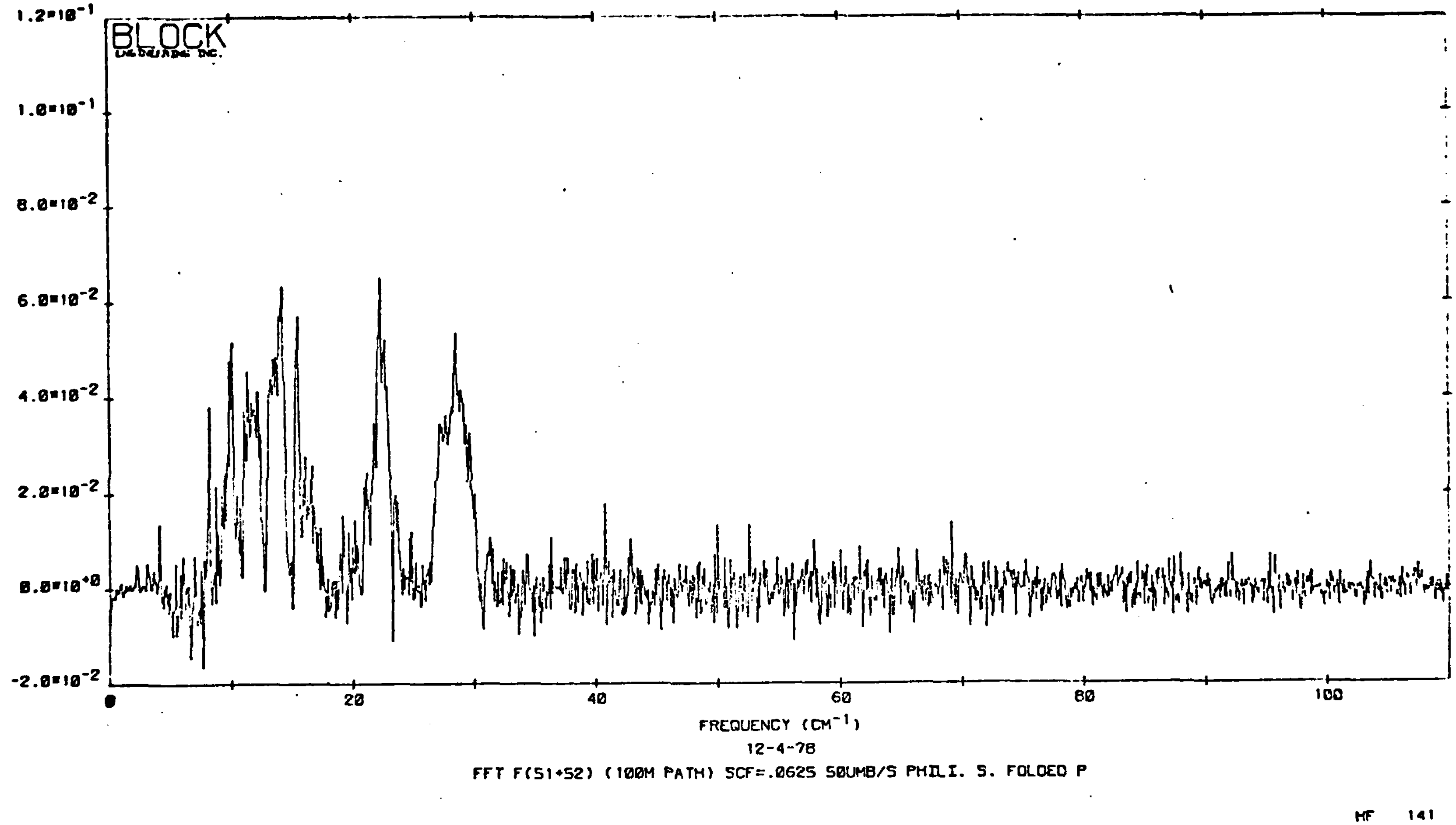

Figure 4.1-15. 100 Meter Spectrum,
90% R.H., 16°C.

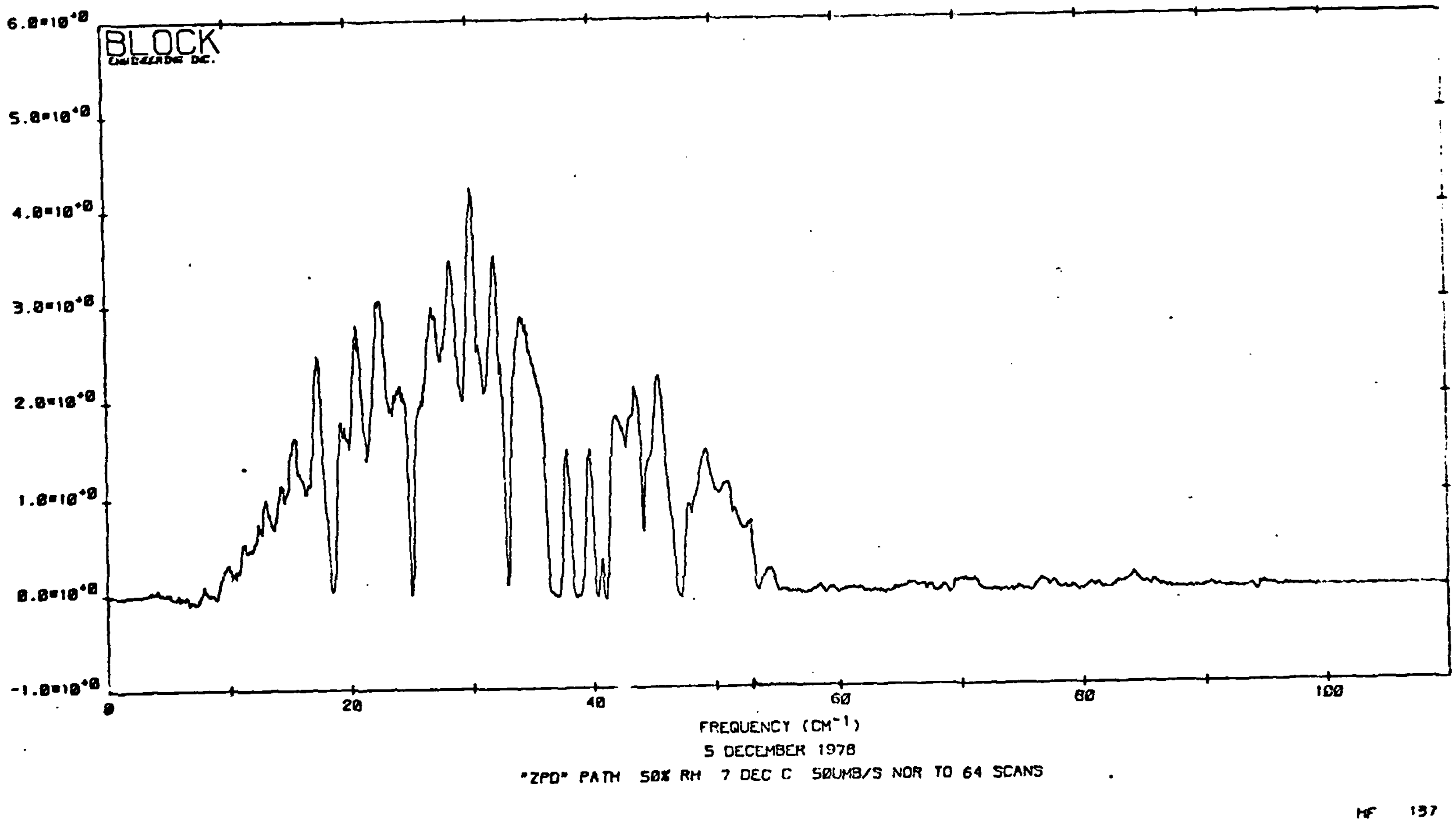

Figure 4.1-16. Zero Path (Folded) Spectrum
50% R.H., 2°C.

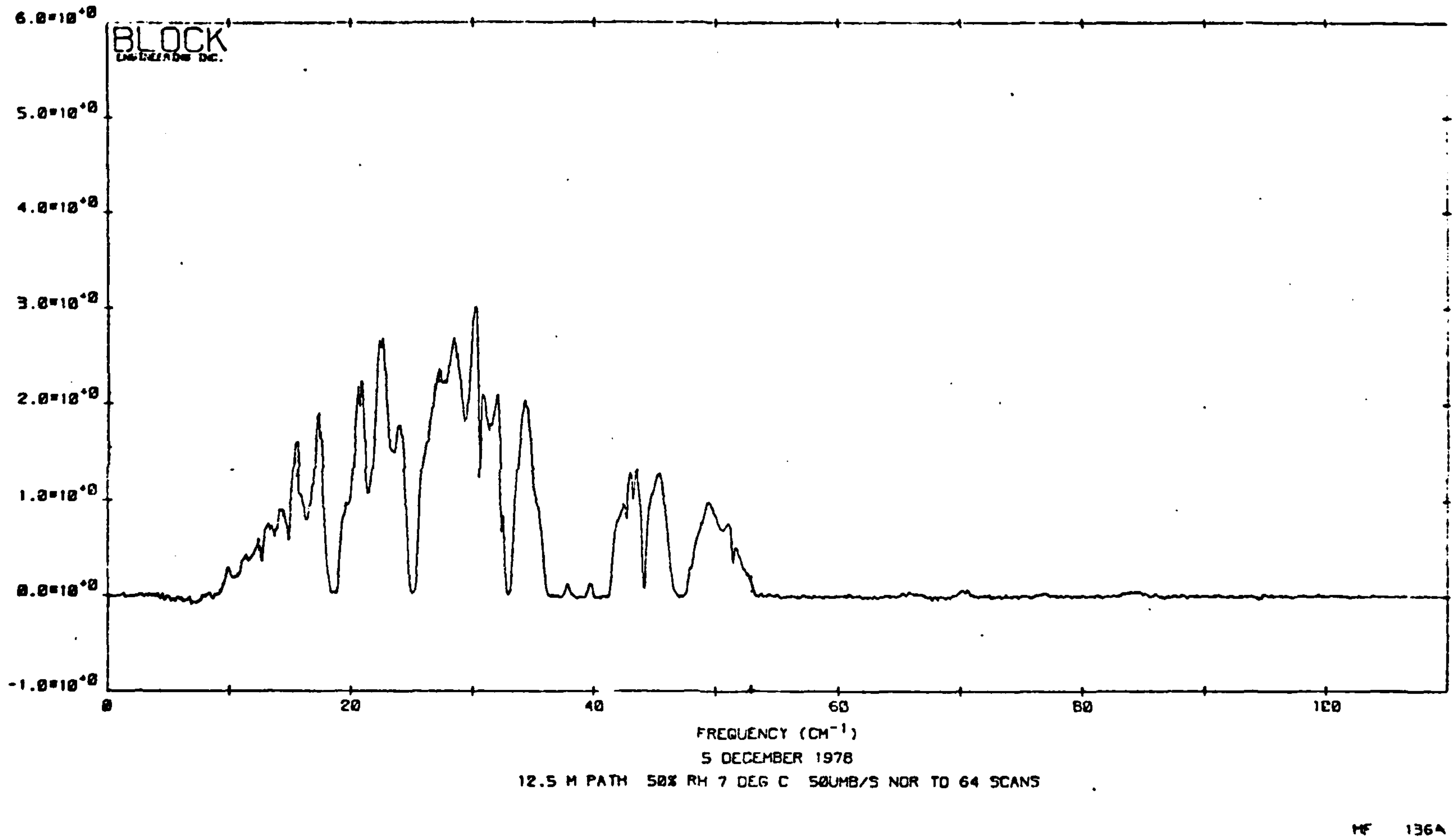

Figure 4.1-17. 12.5 Meter Spectrum, 46% R.H., 3°C.

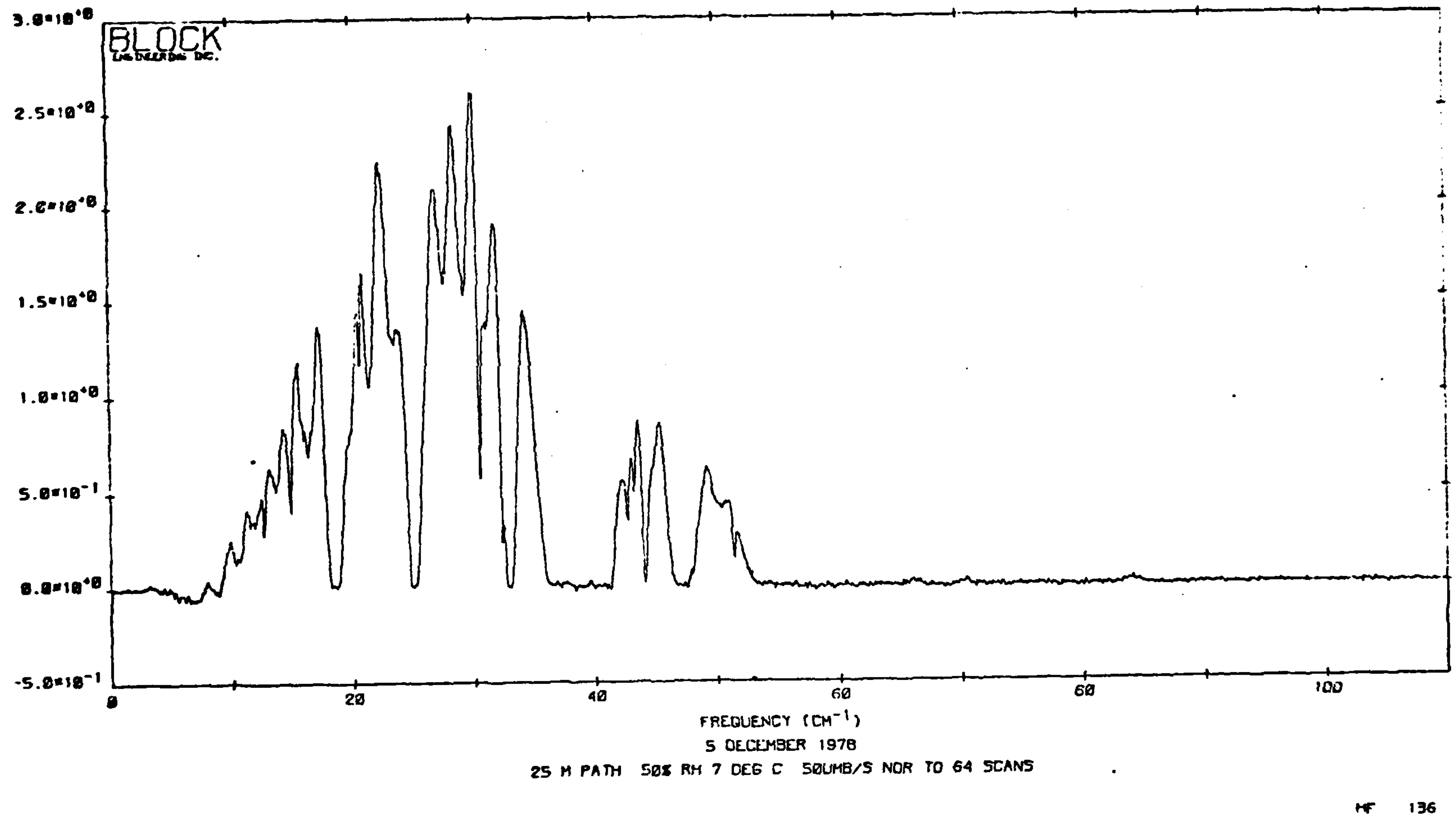

Figure 4.1-18. 25 Meter Spectrum,
46% R.H., 3°C.

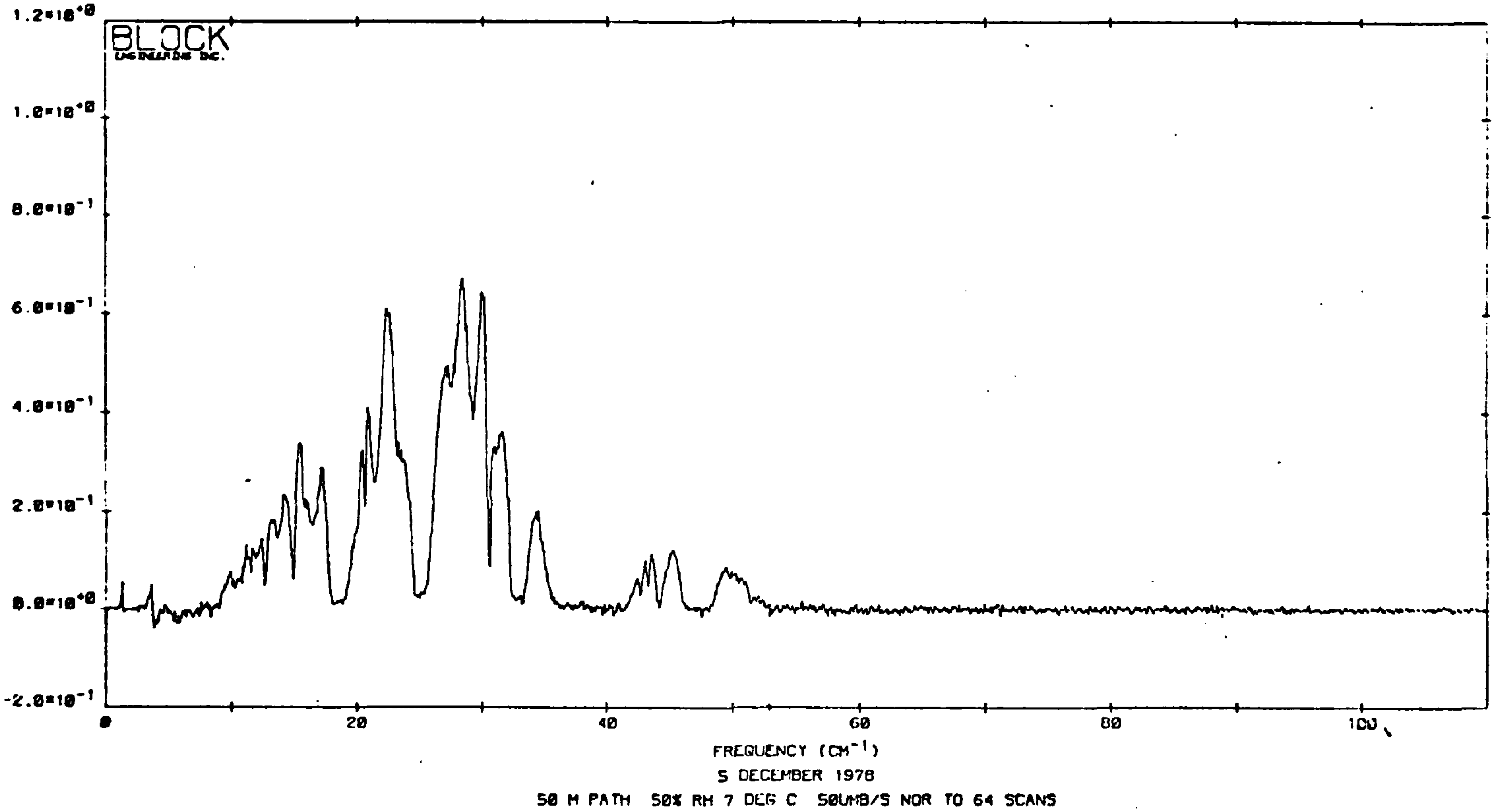

Figure 4.1-19. 50 Meter Spectrum, 39% R.H., 4°C.

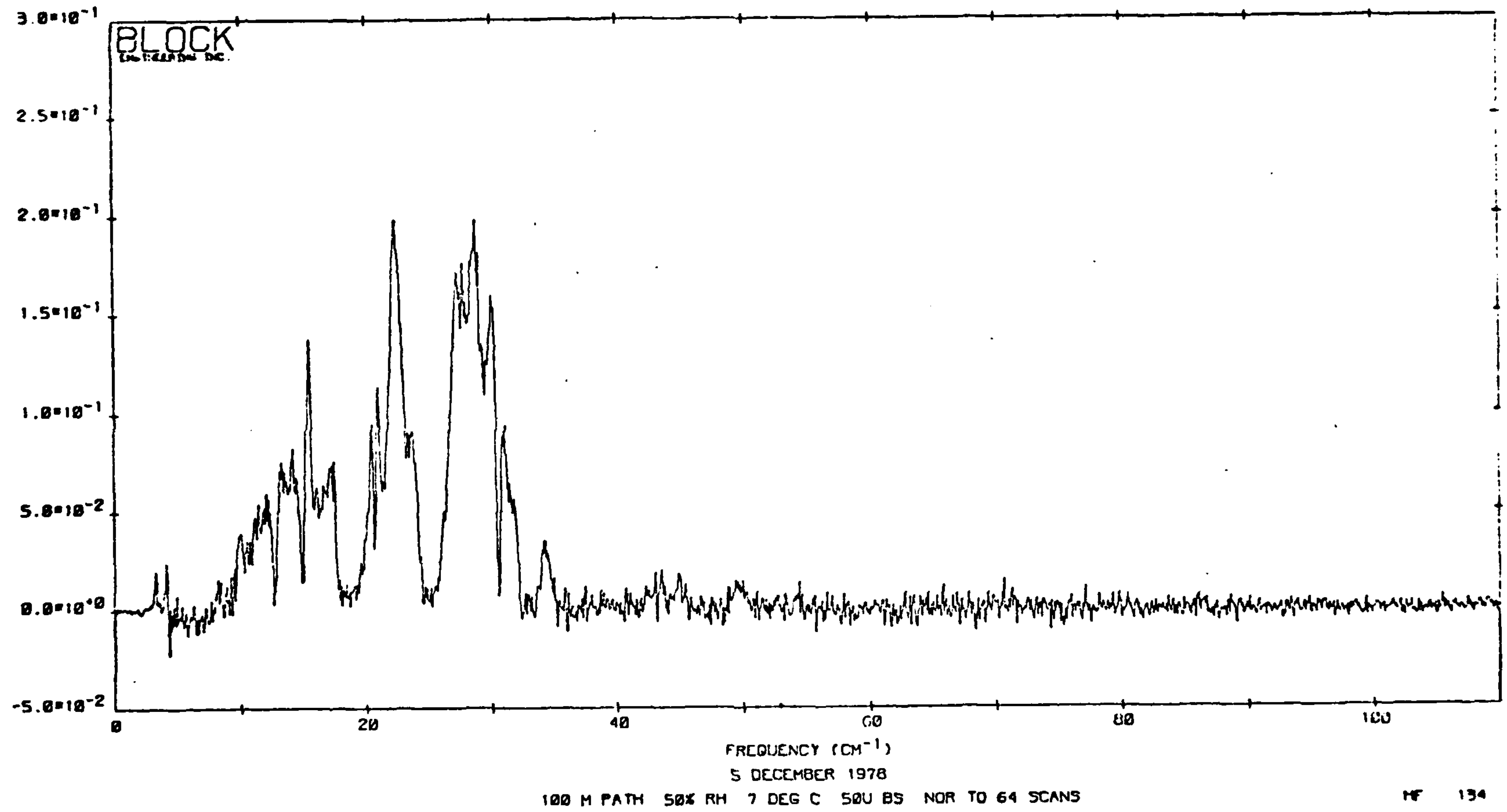

Figure 4.1-20. 100 Meter Spectrum, 39% R.H., 4°C.

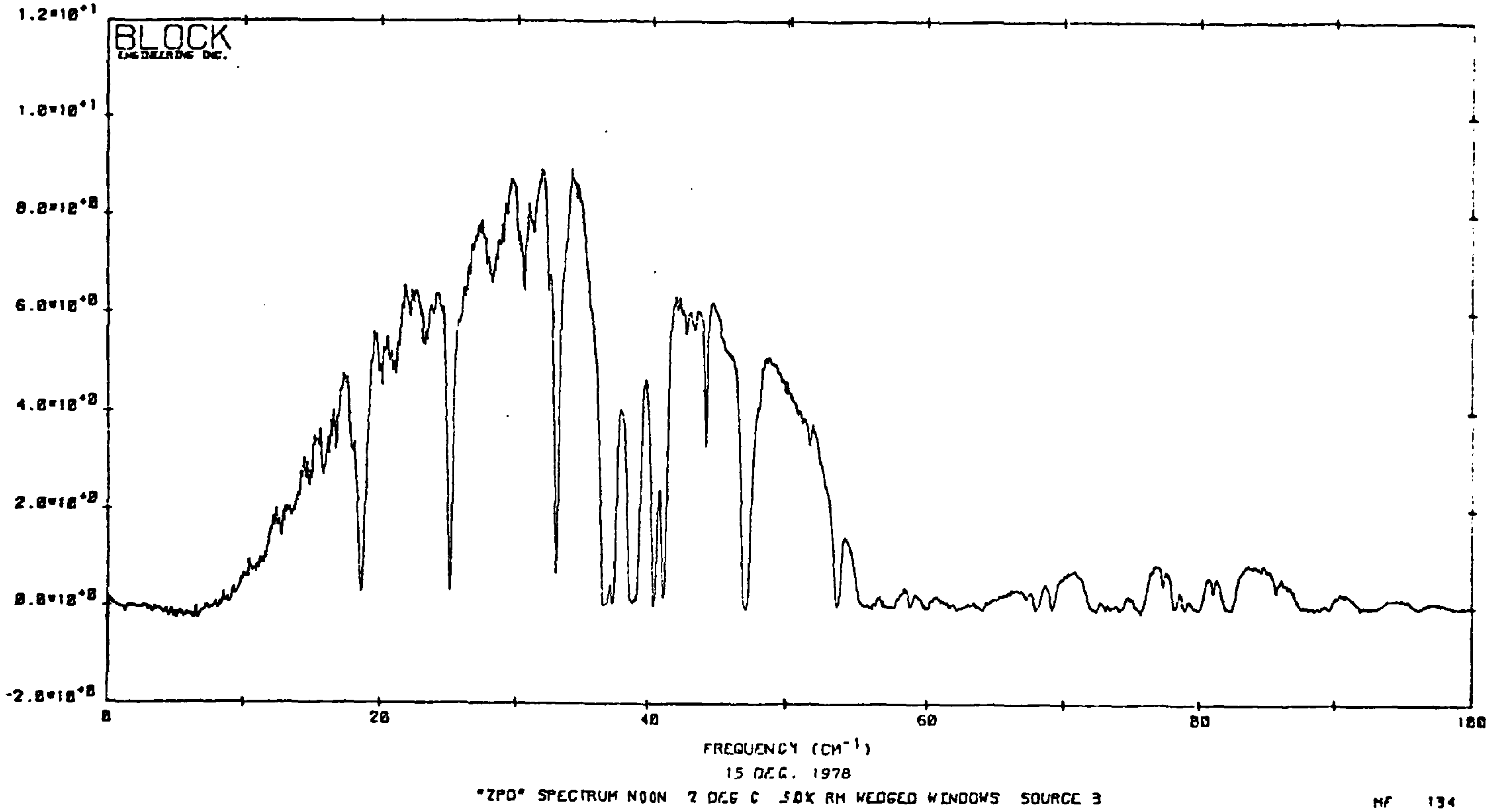

Figure 4.1-21. Zero Path (Folded) Spectrum, 50% R.H., 4°C.

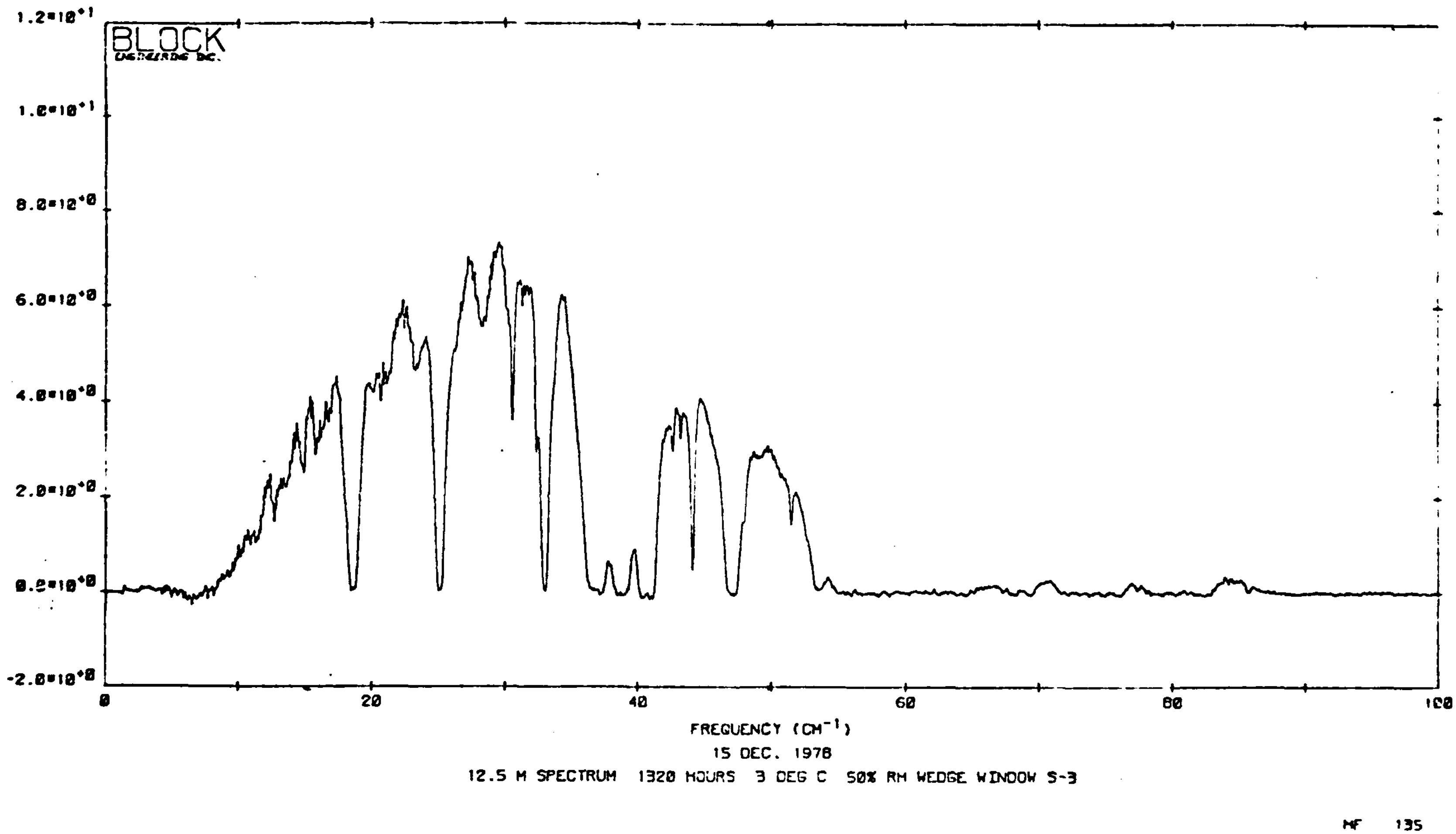

Figure 4.1-22. 12.5 Meter Spectrum, 50% R.H., 3°C.

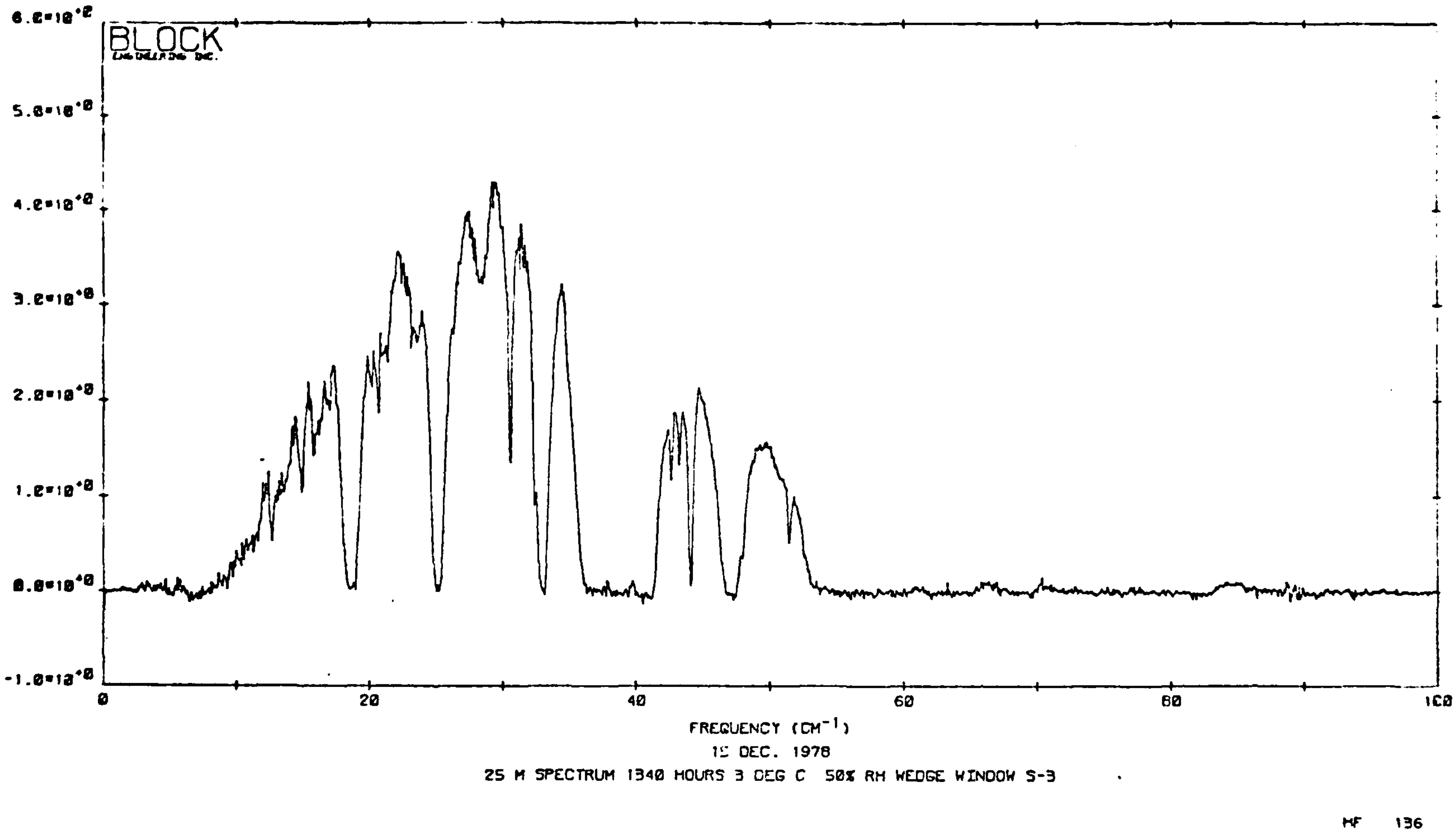

Figure 4.1-23. 25 Meter Spectrum,
46% R.H., 3°C.

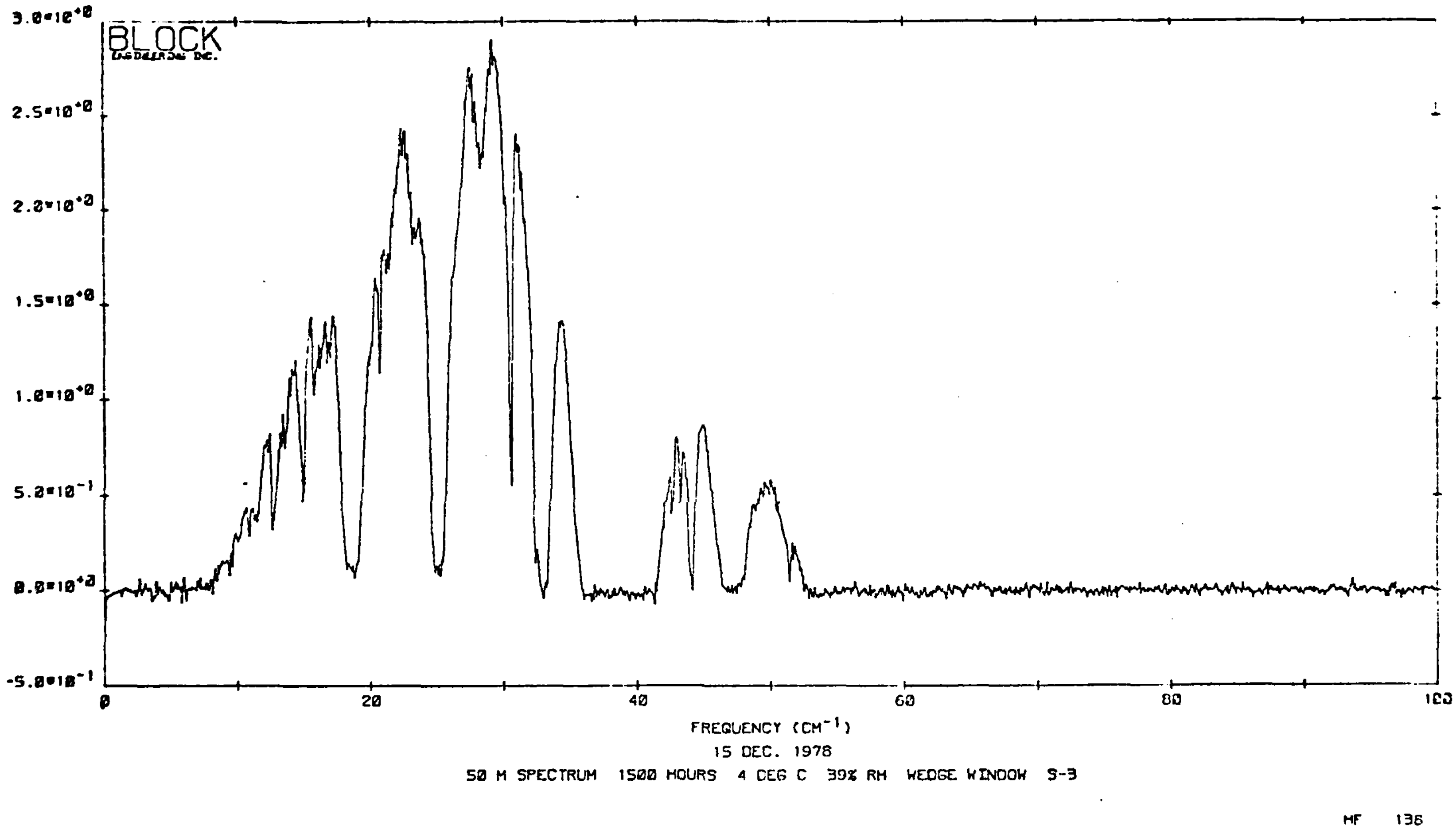

Figure 4.1-24. 50 Meter Spectrum,
39% R.H., 4°C.

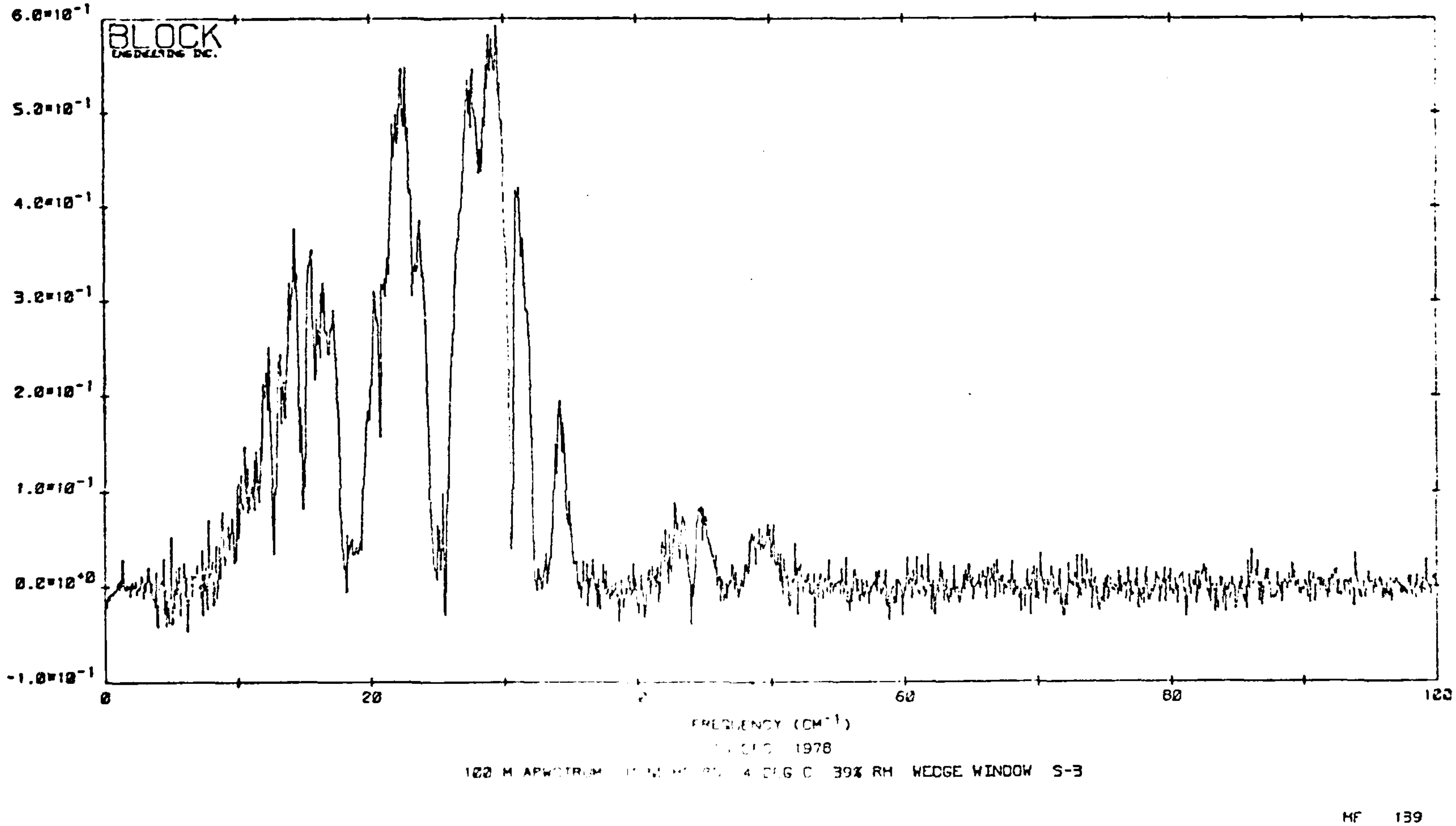

Figure 4.1-25. 100 Meter Spectrum, 39% R.H., 4°C.

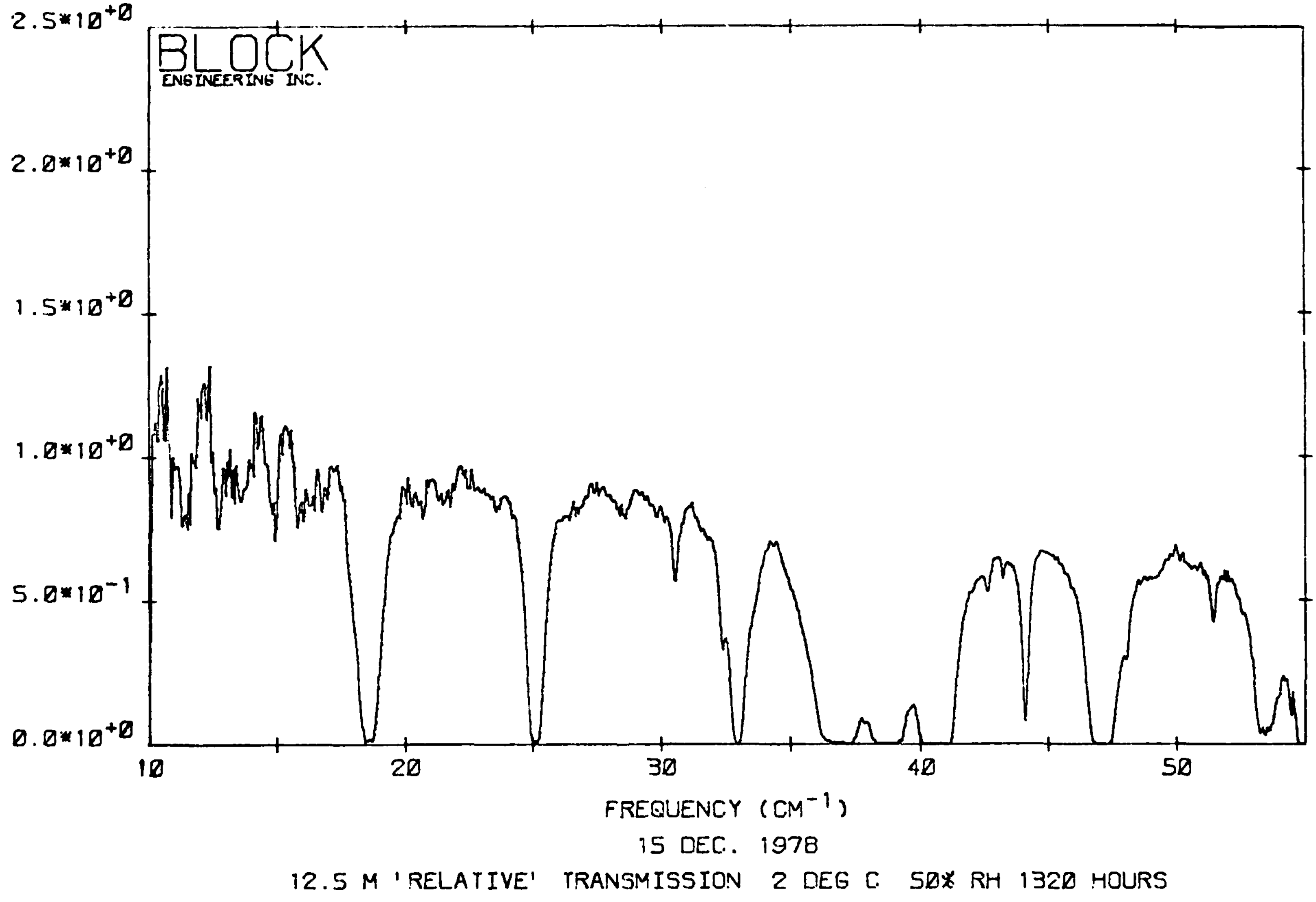

Figure 4.1-26. 12.5 Meter Ratio, 46% R.H., 3°C.

VF 145

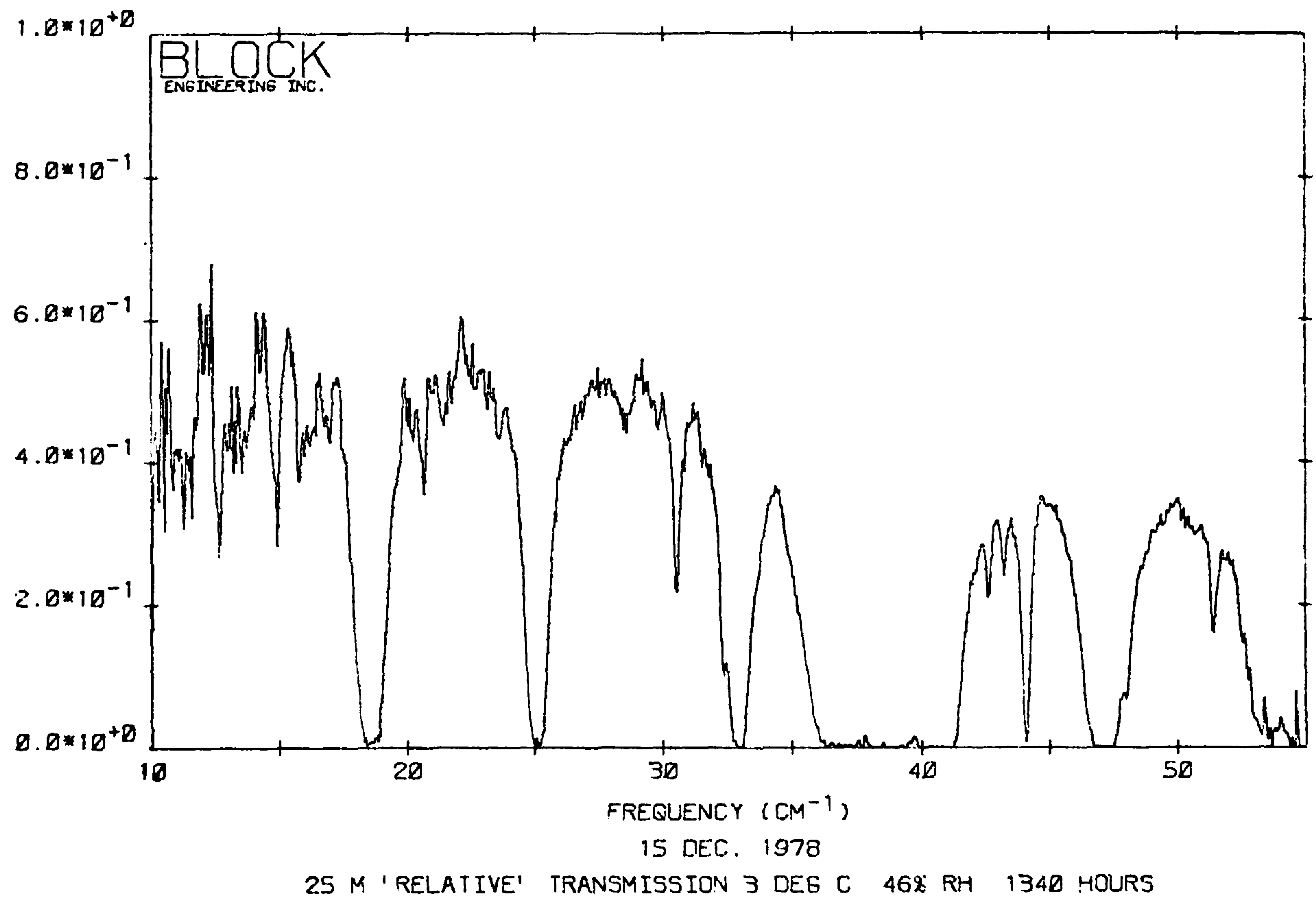

Figure 4.1-27. 25 Meter Ratio, 46% R.H., 3°C.

VF 144

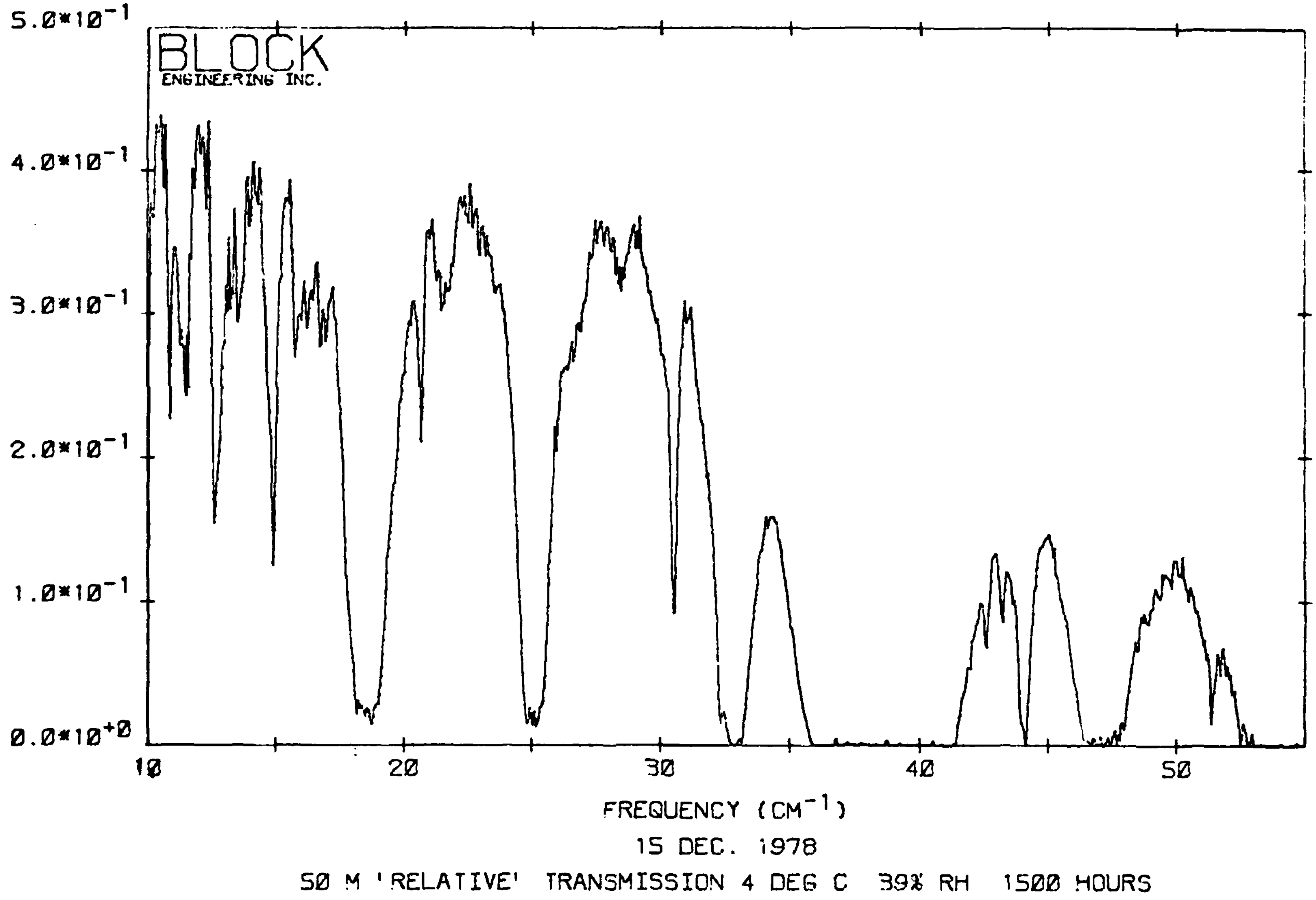

Figure 4.1-28. 50 Meter Ratio, 39% R.H., 4°C.

VF 143

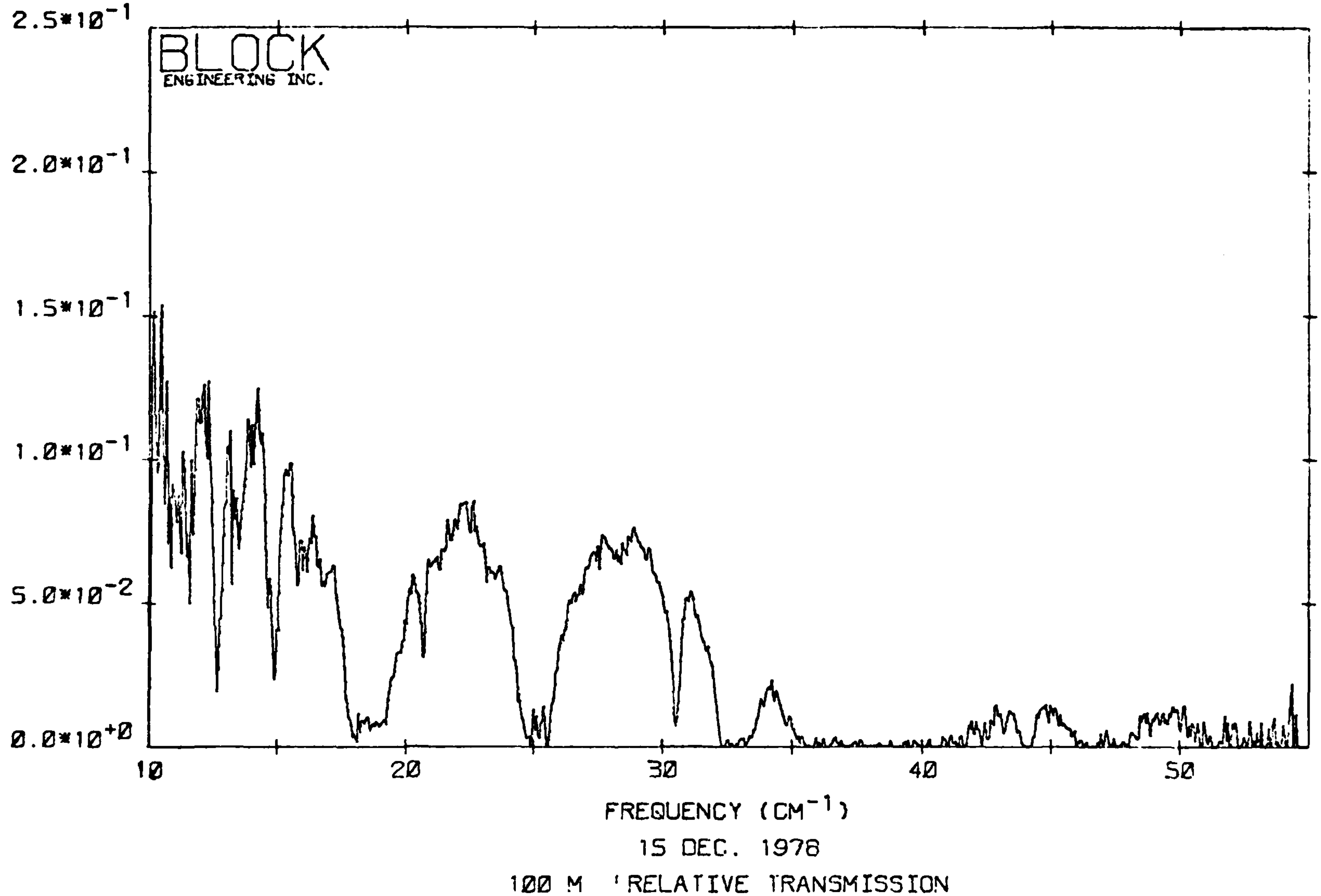

Figure 4.1-29. 100 Meter Ratio, 37% R.H., 4°C.

VF 142

4.2 DISCUSSION

In general, the absorption of water vapor dominates the spectrum throughout the measured region. Water bands were noted at the specific positions indicated in Table 4.2-I, and three bands were noted which could not be assigned. These three bands are not water absorption bands, as can be seen by comparing 50 meter path spectra at 39% and 97% relative humidities, observing that the bands disappear in ratioing these data. It is possible that the features at 11.5 cm^{-1} may be related to the CO line at 11.6 cm^{-1}, but the band seems clearly offset from this position. The band at 21.5 cm^{-1} coincides with a channeling dip in the earlier spectra, however, it is generally present in the spectra obtained with a wedged filter, which do not show any significant indications of channeling. The bands at 11.5 cm^{-1} and 13.6 cm^{-1} are more sharply defined, and do not fit into channel dips in a consistent way. The 13.6 cm^{-1} band does not coincide with lines noted by Harries (1972) or Fleming and Chamberlain (1974) although an N_2O line is present at 13.4 cm^{-1} in the latter data.

No clear indications were noted of anomalous absorption due to water dimers, as discussed by Harries (1972) or Gebbie et al (1968). Some indications are present in the data of increasing absorption below 10 cm^{-1}, but the decrease in signal-to-noise makes this data suspect. The transmission from 22 cm^{-1} to 25 cm^{-1} does not appear to be profoundly affected by the increased humidity in comparing Figures 4.1-12 through 4.1-15 with Figures 4.1-17 through 4.1-20, but there is some unusual variation in band shape. Unfortunately, the increased noise in Figure 4.1-15 makes the apparent line at 23.2 cm^{-1} of dubious significance.

The general quality of the spectra, however, is excellent, even in the cases where channeling is present. We note that reported measurements by Gimmestad et al (1977) and Moffat et al (1977) show channeling, although of somewhat reduced level. It is possible that some channeling is still present with the wedged filters, but we estimate that it is less than 3% of the spectral irradiance at any point. The channeling in the earlier zero path spectra is variable up to 30%, but this drops to less than 5% in the long path spectra. Lower level absorptions are certainly present in the data, such as O_2 at 12.19 cm^{-1} and 14.17 cm^{-1}, but we have noted only strong absorbers in this limited discussion.

Table 4.2-Ia. Observed Lines/Bands

WAVENUMBER	WAVELENGTH	IDENTIFICATION	REFERENCE
10.86 cm^{-1}	920.8 microns	H_2O	10.85 cm^{-1}
11.5	870.	Unknown, possibly CO	11.60
12.60	793.7	H_2O	12.68
13.6	735.0	Unknown	
14.92	670.2	H_2O	14.92
15.78	633.7	H_2O	15.68/15.87
18.52	540.0	H_2O	18.58
20.78	481.2	H_2O	20.71
21.5	465.0	Unknown	
25.09	398.6	H_2O	25.09
28.56	350.1	H_2O	28.31/28.68
30.71	325.6	H_2O	30.56
32.92	303.8	H_2O	32.94
36.41	274.7	H_2O	36.59
38.50	259.8	H_2O	38.45/38.62
39.97	250.2	H_2O	39.39
40.75	245.4	H_2O	40.8
42.93	232.9	H_2O	42.6
43.56	229.6	H_2O	43.3
44.44	225.0	H_2O	44.0
46.70	214.1	H_2O	46.9

Table 4.2-Ib. Observed Lines/Bands (Concluded)

WAVENUMBER	WAVELENGTH	IDENTIFICATION	REFERENCE
51.77 cm^{-1}	193.2 microns	H_2O	51.4 cm^{-1}
53.48	187.0	H_2O	53.4
55.8	179.0	H_2O	55.7
57.3	175.0	H_2O	57.2
58.9	170.0	H_2O	58.8
60.0	167.0	H_2O	59.9
68.2	147.0	H_2O	68.1
69.4	144.0	H_2O	69.2
72.2 - 74.3	135.0 - 139.0	H_2O	72.2/73.1/74.1
75.7	132.0	H_2O	75.5
77.3	129.0	H_2O	77.4
78.2	128.0	H_2O	78.1
79.0	127.0	H_2O	78.9
79.7	126.0	H_2O	79.7
81.1	123.0	H_2O	80.9
82.3	122.0	H_2O	82.1
85.6	117.0	H_2O	85.6
87.5 - 89.4	112.0 - 114.0	H_2O	88.0/88.8/89.4
91.9 - 93.1	107.0 - 109.0	H_2O	92.6
96.2	104.0	H_2O	96.1

5. CONCLUSIONS

Atmospheric transmission has been measured at 0.1 cm^{-1} spectral resolution over paths of 12.5, 25, 50 and 100 meters. Data were obtained that show the effects of variable humidity between 39% and 97% relative humidity. Relative transmission ratios were obtained for moderate humidity conditions. Spectral quality was generally excellent, although increasing absorption at shorter wavelengths and with increasing humidity resulted in increased noise there. Although we had hoped to extend the spectral range beyond one millimeter wavelengths, the system response fell off too rapidly to allow this, and limited financial resources and time prevented further improvement in the instrumentation. This also prevented taking the apparatus to a fully instrumented meteorological station.

5.1 FURTHER MEASUREMENTS

The next step in an extended atmospheric characterization program can be the improvement of instrumentation, extending the spectral response beyond one millimeter and enabling the accurate calibration of the spectra to provide absolute transmission over the expanded spectral range. The equipment should be taken to an instrumented meteorological station, set up in a semi-permanent configuration, and operated intermittently over an extended period of time to include a wide range of atmospheric conditions. A less expensive alternative is the installation of the equipment at the Block Engineering location with a weather station added, perhaps using government-furnished apparatus. It would be most desirable to provide a mathematical modeling capability in parallel with the measurement program, either through the sponsoring agency or through Block Engineering, which has full computer capability for such work, including use of LOWTRAN and HITRAN computer programs.

5.2 INSTRUMENT MODIFICATIONS

The spectral response of the transmitter is limited at longer wavelengths by diffraction in the transmitter telescope and by interference effects in the dielectric beamsplitter. The diffraction effects are relatively minor, providing an eight milliradian field at 2.0 mm. At wavelengths approaching 0.5 cm, however, this telescope should be replaced by one with an aperture size increased to at least 24 inches diameter.

High quality optical surfaces are not necessary, and an inexpensive metal mirror telescope would be quite satisfactory.

The loss in efficiency for the film beamsplitter can be totally eliminated by the use of wire grid beamsplitters in the Martin and Puplett configuration. A loss of 50% in efficiency is experienced because one polarization is lost, but the efficiency is uniform from the short wavelength limit to the longest wavelengths which can pass through the system. The incorporation of an improved beamsplitter is considered essential to extending the long wavelength response, and the periodic nulls and erractic partial polarization in thick film beamsplitters are considered an additional reason for preferring the wire grid type.

The 8.0 inch diameter receiver telescope is clearly too small, making accurate calibration virtually impossible with a larger transmitter telescope. Ideally, the receiver telescope should be as large or larger than the transmitter telescope, and the most satisfactory technique is that in which the entire transmitted beam is intercepted by the receiver at every range. The width of beam for a 24 inch transmitter at 2 mm is 4 milliradians, giving a focused diameter of 15.7 inches at 100 meter range. A receiver telescope 24 inches in diameter would suffice in this case. At 5 mm, however, this beam becomes 10 milliradians wide, with a focused diameter of 39.4 inches at 100 meters. Increasing both transmitter and receiver diameters to 36 inches gives a 6.7 mr beam, and focused diameter of 26 inches at the receiver, allowing some alignment tolerance. Inexpensive metal mirrors can be obtained to 36 inches in diameter.

The spectral limit in the receiver comes from the detector and its associated optics. The present detector is 3.0 mm square, at the focus of a 6.0 mm diameter field lens. This constitutes a significant loss at wavelengths beyond 2-3 mm, due to the inefficient coupling of radiation into the detector and the increasing diffraction effects in the optics. Modification of the optics will be necessary in going to a larger receiver telescope in any case, since the throughput (area-solid angle product) must also increase with the extension to longer wavelengths, apart from detector and coupling optic considerations.

The extent and complexity of instrument modification depends on the degree of extension of spectral response and the precision required in calibration. A set of measurements made at fixed range, with all components locked in position, can be made over the present spectral range without modification at all. Adjusting the clear weather spectra for computed

absorption, or even covering the entire path with a purged plastic shroud will permit a reasonably accurate correction to zero air mass.

The incorporation of accurate meteorological data into the measurement program is essential. As a minimum, local temperature, relative humidity, pressure, visibility, and precipitation measure are needed . Detailed measurement of particulates would be of great value, provided that water aerosols can be monitored accurately.

5.3 MEASUREMENT SCHEDULING

The logistics of an extended, fixed configuration measurement program are complicated by the requirement for liquid helium supply. Since weather phenomena tend to be difficult to predict, it is necessary to establish probabilities for various phenomena and arrange for helium delivery in advance of high probability time periods. A certain degree of helium loss may be expected in waiting for acceptable weather conditions, however, this loss can be minimized by good planning or by installation of a high efficiency storage dewar at the site. Since the latter can be quite expensive, we believe that careful and detailed planning of measurements based on projected weather patterns will be the best approach.

The weather conditions of greatest interest include fog, rain, and snow, with the most signficant measurements probably being at the point of incipient precipitation. A three month program will give a high probability for these conditions, but planning must be flexible and coordinated on a week-by-week basis during the program.

Operation at a site remote from Block's Cambridge facility would require tape recording of spectral data and careful log keeping for meteorological data. These tape records can be played back at Block for computer processing at any time, but it is desirable that spectra become available as soon as possible so that system performance can be monitored. Thus, the measurement schedule should include coordination with data processing experts at Block on the same week-by-week basis. The committment of these persons to the program is increased, of course, if computer modeling is also being carried out here.

BIBLIOGRAPHY

Bastin, J. A., "Extreme Infra-Red Atmospheric Absorption," Infrared Phys., 6, 209, 1966.

Burch, D. E., "Absorption of Infrared Radiant Energy by CO_2 and H_2O. III. Absorption by H_2O between 0.5 and 26 cm^{-1}," Jnl. Opt. Soc. Am., 58, 1383, 1968.

Burroughs, W. J., Pyatt, E. C., Gebbie, H. A., "Transmission of Sub-Millimeter Waves in Fog," Nature, 212, 387, 1966.

Carlon, H. R., "Phase Transition Changes in the Molecular Absorption Coefficient of Water in the INfrared: Evidence for Clusters," Appl. Opt., 17, 3192, 1978.

Emery, R., "Atmospheric Absorption Measurements in the Region of 1 mm Wavelength," Infrared Phys., 12, 65, 1972.

Fleming, J. W., Chamberlain, J., "High Resolution Far Infrared Fourier Transform Spectrometry Using Michelson Interferometers with and without Collimation," Infrared Phys., 14, 277, 1974.

Gebbie, H. A., Burroughs, W. J., "Observations of Atmospheric Absorption in the Wavelength Range 2 mm to 300 um," Nature, 217, 1241, 1968a.

Gebbie, H. A., Chamberlain, J., Burroughs, W. J., "Sub-Millimetre Wave Solar Observations," Nature, 220, 893, 1968b.

Gebbie, H. A., Burroughs, W. J., Chamberlain, J., Harries, J. E., Jones, R. G., "Dimers of the Water Molecule in the Earth's Atmosphere," Nature, 221, 143, 1969.

Gimmestad, G. G., Gebbie, H. A., "Atmospheric Absorption in the Range 12 cm^{-1} to 32 cm^{-1} Measured in a Horizontal Path, Jnl. Atmospheric and Terrestrial Phys., 38, 325, 1976.

Gimmestad, G. G., Ware, R. H., Bohlander, R. A., Gebbie, H. A., "Observations of Anomalous Submillimeter Atmospheric Spectra," Astrophysical Journal, 218, 311, 1977.

Harries, J. E., Burroughs, W. J., "Observations of Millimetre Wavelength Solar Radiation at Sea Level," Infrared Phys., 10, 165, 1970.

BIBLIOGRAPHY
(Continued)

Harries, J. E., Ade, P. A. R., "The High Resolution Millimeter Wavelength Spectrum of the Atmosphere," Infrared Phys., 12, 81, 1972.

Harries, J. E., "Absorption by Minor Atmospheric Constituents Near 8 cm^{-1}," Infrared Phys., 12, 143, 1972.

Moffat, P. H., Bohlander, R. A., Macrae, W. R., Gebbie, H. A., "Atmospheric Absorption Between 4 and 30 cm^{-1} Measured above Mauna Kea," Nature, 269, 676, 1977.

LMED

–8